

SEMI-ANNUAL REPORT NO. 5
DECEMBER 1966

FACILITY FORM 602

N 68-18166 (ACCESSION NUMBER) (THRU)

13 (PAGES)

OL-81721 (NASA CR OR TMX OR AD NUMBER) (CODE)

17 (CATEGORY)

CREEP AT ELEVATED TEMPERATURES
AND HIGH VACUUM

GPO PRICE \$ _____

CFSTI PRICE(S) \$ _____

BY Hard copy (HC) 3.00

Microfiche (MF) 1.65

ff 653 July 65

K. SCHRÖDER, A. GIANNUZZI AND G. GORSHA

This report was produced under a sponsored contract. The conclusions and recommendations expressed are those of the Author(s) and are not necessarily endorsed by the Sponsor. Reproduction of this report, or any portion thereof, must bear reference to the original source and Sponsor.

SYRACUSE UNIVERSITY RESEARCH INSTITUTE

DEPARTMENT OF CHEMICAL ENGINEERING AND METALLURGY

Approved by:

K. SCHRÖDER

K Schröder

Sponsored by:

OFFICE OF RESEARCH GRANTS
AND CONTRACTS - NATIONAL
AERONAUTICS AND SPACE
ADMINISTRATION

S.U.R.I. Report No.

MET. E. 1189-1266-SA

Date:

DECEMBER 1966

TABLE OF CONTENTS

	PAGE
ABSTRACT	i
I. INTRODUCTION	1
II. EXPERIMENTAL PROCEDURE AND RESULTS	4
REFERENCES	6
FIGURES	7
III. APPENDIX - M. S. THESIS OF A. GIANNUZZI <i>Removed.</i>	

ABSTRACT

Creep tests in high vacuum and elevated temperatures were continued on copper of 99.9% purity and silver of 99.999% purity. The testing procedure was unchanged, and the experimental results were analogue to previously obtained data: the minimum creep rate decreased, if an initially argon bombarded and tested sample was annealed in air and retested in the same vacuum and temperature.

Such results are surprising. A silver sample should interact at elevated temperatures with air quite differently than copper, because silver oxide is not stable in our testing conditions, whereas copper samples showed quite strong oxide films. It is therefore more likely, that the reduction of the creep rate is not due to an oxide film. It is more likely associated with the absorption of oxygen in the sample, where it may either harden grain boundaries, retard the operation of dislocation sources, or increase frictional forces on moving dislocations. It is also possible that a partial oxygen monolayer could interfere with slip line formation.

INTRODUCTION

Studies of the plastic deformation of metals have shown, that a vacuum environment affects the mechanical strength of metals¹⁻⁴. (A more detailed discussion of relevant literature is given in Appendix A, which contains the draft of Mr. Giannuzzi's M.S. thesis.) The strength can both increase or decrease if tested in vacuum. Such strength changes are frequently explained with the structure of surface films. It has been, for instance, proposed, that an oxide layer on the sample surface could weaken the specimen. Sweetland and Parker² proposed that an oxide film acts sometimes in a similar way as grain boundaries, or as a large second phase inclusion in the matrix. They suggest that such an oxide layer may operate as a dislocation source. One would expect that this would weaken the sample. Another weakening mechanism may be due to crack formation of the brittle oxide film. Such cracks act as stress raisers, and may be responsible for excessive plastic flow in the sample. This may be important for the initiation of necking, the last stage of creep before fracture.

Most experimental evidence indicates, however, that the surface defects strengthen the sample. For instance, continuous removal of surface layers by electrolysis produced a marked decrease in the work hardening rate⁴.

Our experiments on the creep rate of high purity copper (99.999%) showed corresponding effects³. The minimum creep rate, after an oxidation treatment of the unloaded sample, decreased markedly, if the sample was retested at a similar pressure and temperature as in the first part of the test before oxidation. Several mechanisms have been proposed in the literature, to explain such hardening (see Appendix A), as for instance the concept of a "debris layer"⁴, or dislocation pile-ups on interfaces as surface films⁵. No model

has been found, however, to explain all phenomena.

Most experiments on high vacuum effects are evaluated by correlating high vacuum test results with corresponding tests executed in air. In our measurements, two creep curves, obtained in a high vacuum on one sample, are compared. Changes in the sample should be attributed only to the annealing process between the two tests, not to variations in the creep test environment. This should make it easier to analyze our data.

Our experimental approach has also the advantage that it may help in correlating some high vacuum testing results with the behavior of outer space service condition. Metals in trans-lunar orbits will be exposed to radiation and micrometeoroids, which will strip the metal of protective surface films. This would correspond to a high vacuum test of a sample cleaned by argon bombarding. The second part of the creep test on the oxidized sample in high vacuum would correspond to a "normal" high vacuum test (no surface preparation in ultra clean conditions), and the experiments on 99.999 % Cu copper showed that this "normal high vacuum test" yielded lower minimum creep rates than the identical test on the argon bombarded sample.

It was, however, realized that we have presently no accurate model of our sample surface to conclude with certainty that the high vacuum tests on the argon bombarded sample corresponded to the really well defined "atomically clean surface" state. We therefore initiated tests on silver samples. The solubility of oxygen and nitrogen is very low in both silver and copper⁶. Both are f.c.c. crystals with similar plastic properties. Silver oxide is, however, only stable at atmospheric pressures below 190°C. This means, that no silver oxide would form in our testing conditions. Changes in creep rate

during heating in air could not be due to silver oxide, but would probably be due to diffusion of oxygen into grain boundaries, the silver matrix, or to the interaction of a partial oxygen monolayer with the formation of slip steps. Argon bombarding should remove such oxide monolayer.

The pressure during testing was close to the vapor pressure of the sample in our tests on high purity copper and in silver. We wanted to know if this would influence the creep rate. It seemed possible, that a higher rate of evaporation in tests at higher temperature could affect the slip step formation. It was therefore decided to test copper wires of lower purity under higher loads than in tests with 99.999 % Cu, because preliminary experiments had indicated that similar creep curves could be obtained if 99.9% purity Cu was tested at lower temperatures.

EXPERIMENTAL PROCEDURE AND RESULTS

Only minor changes were incorporated in the vacuum test system. The experimental procedure is essentially the same as before. Appendix A gives a detailed description. The creep curves of 99.9% Cu and 99.999% Ag samples are given in Figures 1 to 5. Details of testing conditions are listed on these Figures. The results are similar as those obtained previously on 99.999% Cu. The minimum creep rate decreases, after the sample has been annealed in air. The only exception seems to be sample no. 3 (see Figure 3). However, the sample fractured so rapidly after reloading that the minimum creep rate could either not be determined, or the stage of minimum creep did not develop, because the sample began to neck at a defect.

Several models have been proposed to explain the influence of surfaces on plastic deformation. These models usually propose, that the surface is stronger than the bulk of the sample. It is possible, that a surface is weaker than the matrix, because dislocations may be emitted easily, and surface irregularities may act as stress raisers. However, elasticity calculations by Head⁵ show that a surface film would retard the egression of dislocations. Kramer suggested from experiments in which the sample surface was removed continually during testing, that a highly stressed layer is usually produced at the surface, which produces a back stress on dislocation sources.

Such models would explain the creep curves on our copper samples. The minimum creep rate of the clean copper sample would be higher than the minimum creep rate of the same sample tested again in vacuum at the same temperature after annealing in air, because the oxide film formed during annealing should form an obstacle for egressing dislocations.

Problems arise with this model, if one tries to explain the creep curves of silver. Silver oxide is not stable under our testing conditions⁶. One could only expect, that a monolayer of oxygen atoms (or a fraction of it) may form on silver, because such monolayers are stable. However, it is difficult to see how such a monolayer could strengthen the crystal considerably. Only small amounts of oxygen can diffuse into the sample because only one monolayer of oxygen atoms at the sample surface is available. It is difficult to see how such a small amount of oxygen can strengthen the sample if it diffuses into the crystal, and strengthens either the grain boundaries, impedes the operation of dislocation sources, or increases frictional forces on moving dislocations.

More experiments are required to clarify these questions.

REFERENCES

1. I. R. Kramer, H. K. Chen and S. E. Podlaseck, Jr., *Exp. Mech.* 6, 23 (1966).
2. E. P. Sweetland and E. R. Parker, *J. Appl. Mech.* 20, 30 (1953).
3. K. Schröder, A. Giannuzzi and G. Gorsha, 4th semiannual report.
4. I. R. Kramer, *Trans. AIME* 233, 1462 (1965).
5. A. K. Head, *Austr. J. Physics* 13, 778 (1962).
6. M. Hansen, *Constitution of Binary Alloys* (McGraw Hill, New York, 1958).

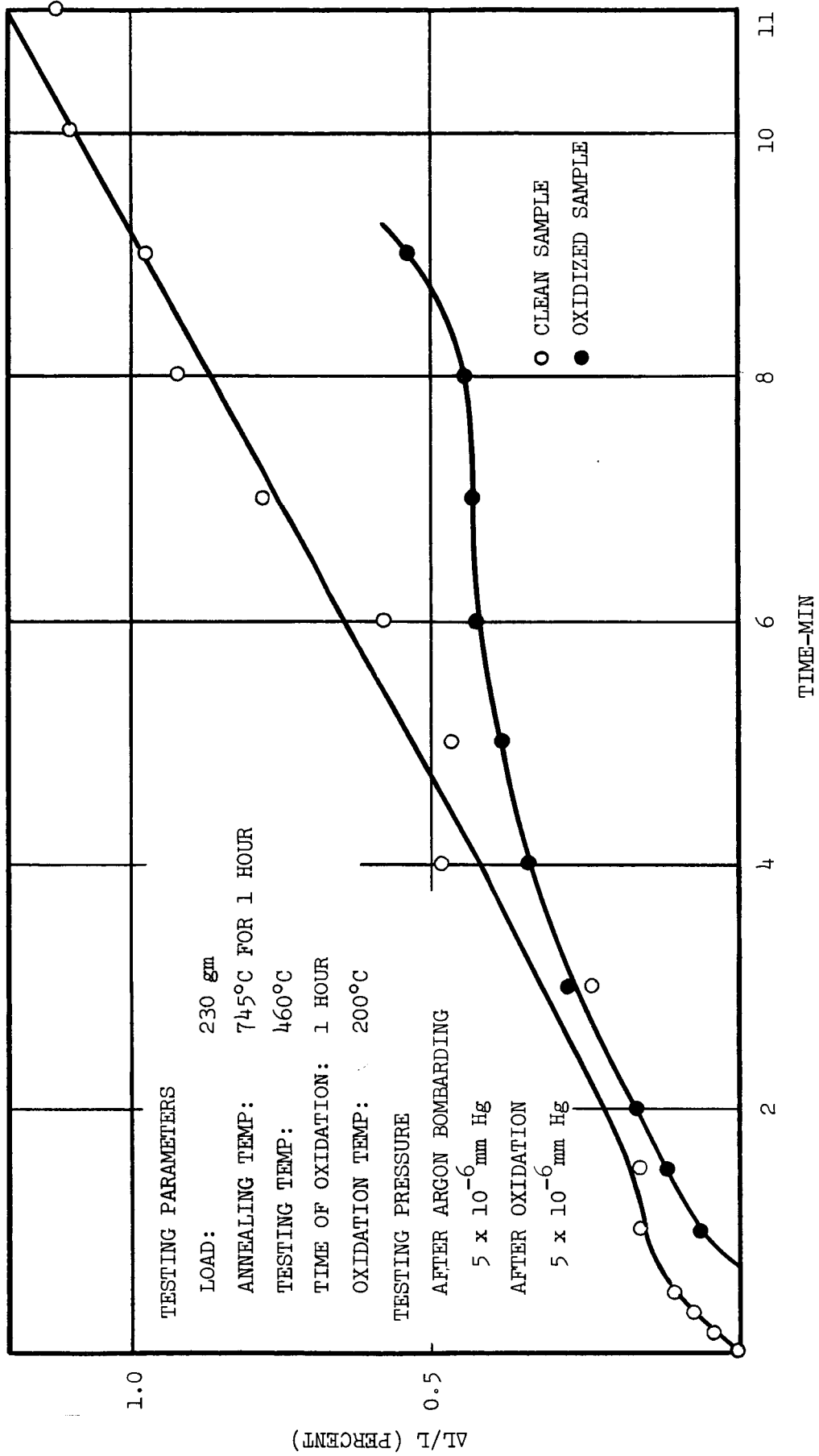


FIG. 1 CREEP TEST OF 0.008 INCH Cu WIRE OF 99.9 PERCENT PURITY

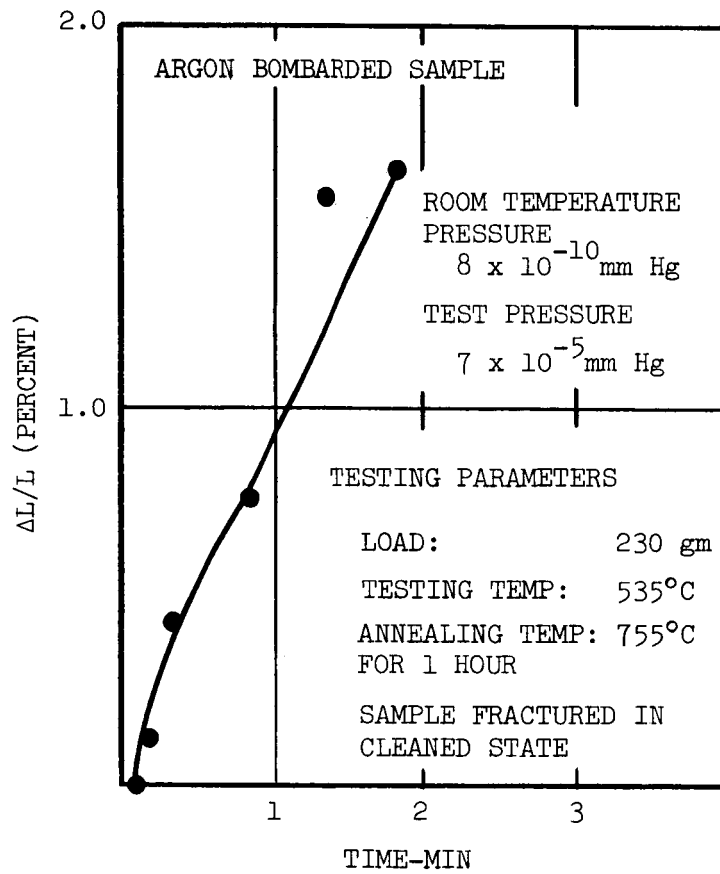


FIGURE 2 CREEP TEST OF 0.008 INCH Cu WIRE OF 99.9 PERCENT PURITY

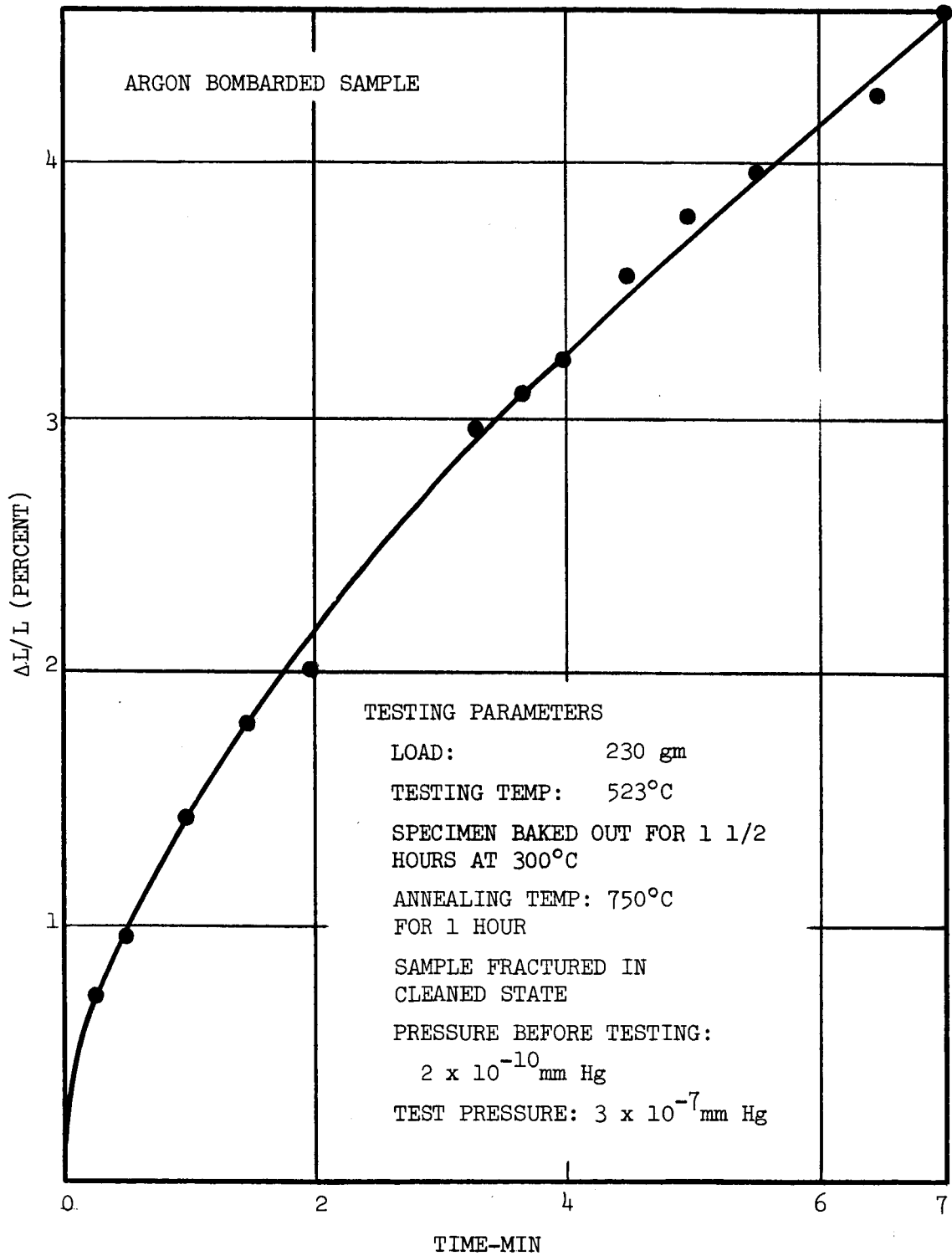


FIGURE 3 CREEP TEST OF 0.008 INCH Cu WIRE OF 99.9 PERCENT PURITY

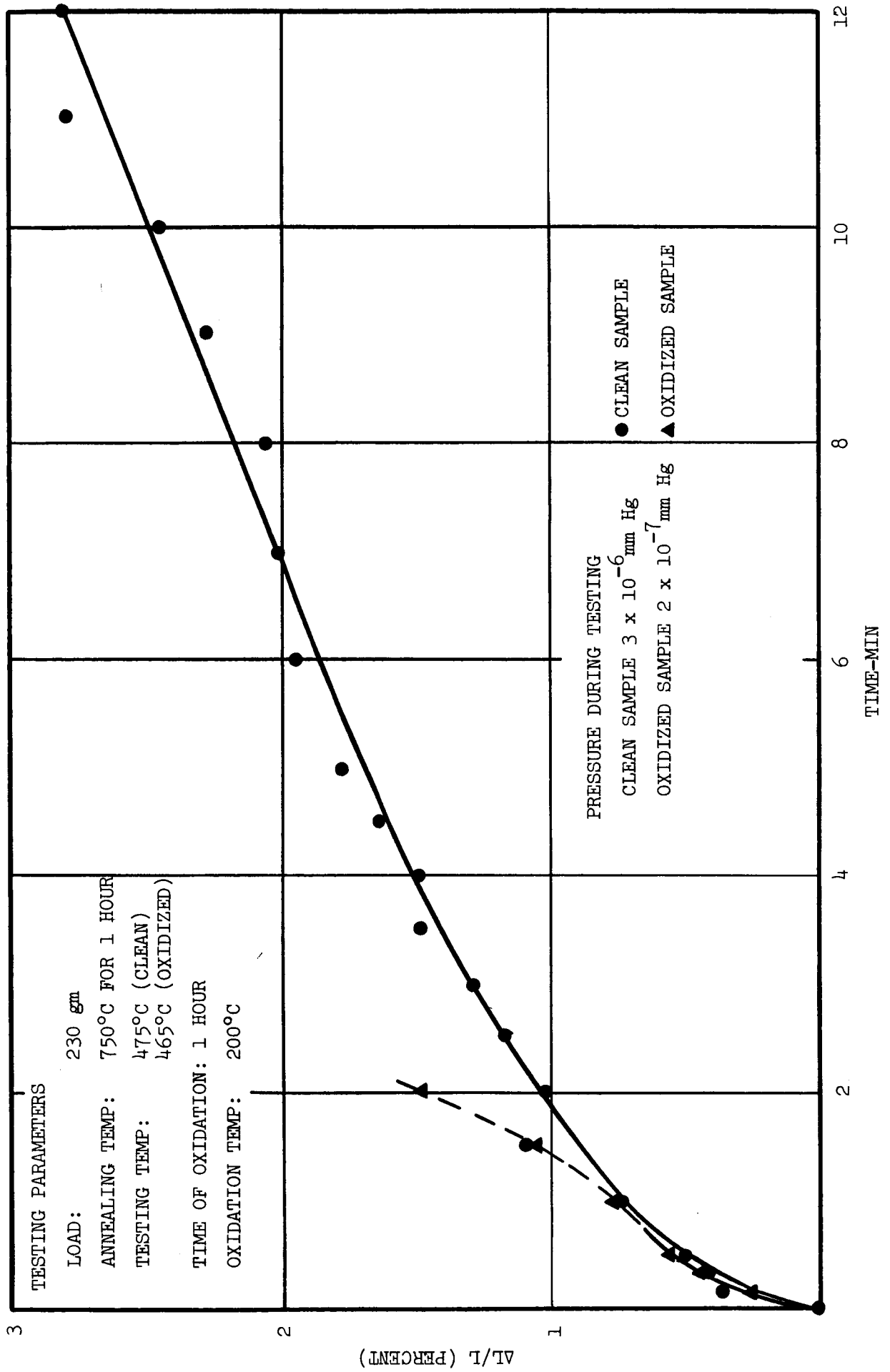


FIG. 4 CREEP TEST OF 0.008 INCH Cu WIRE OF 99.9 PERCENT PURITY

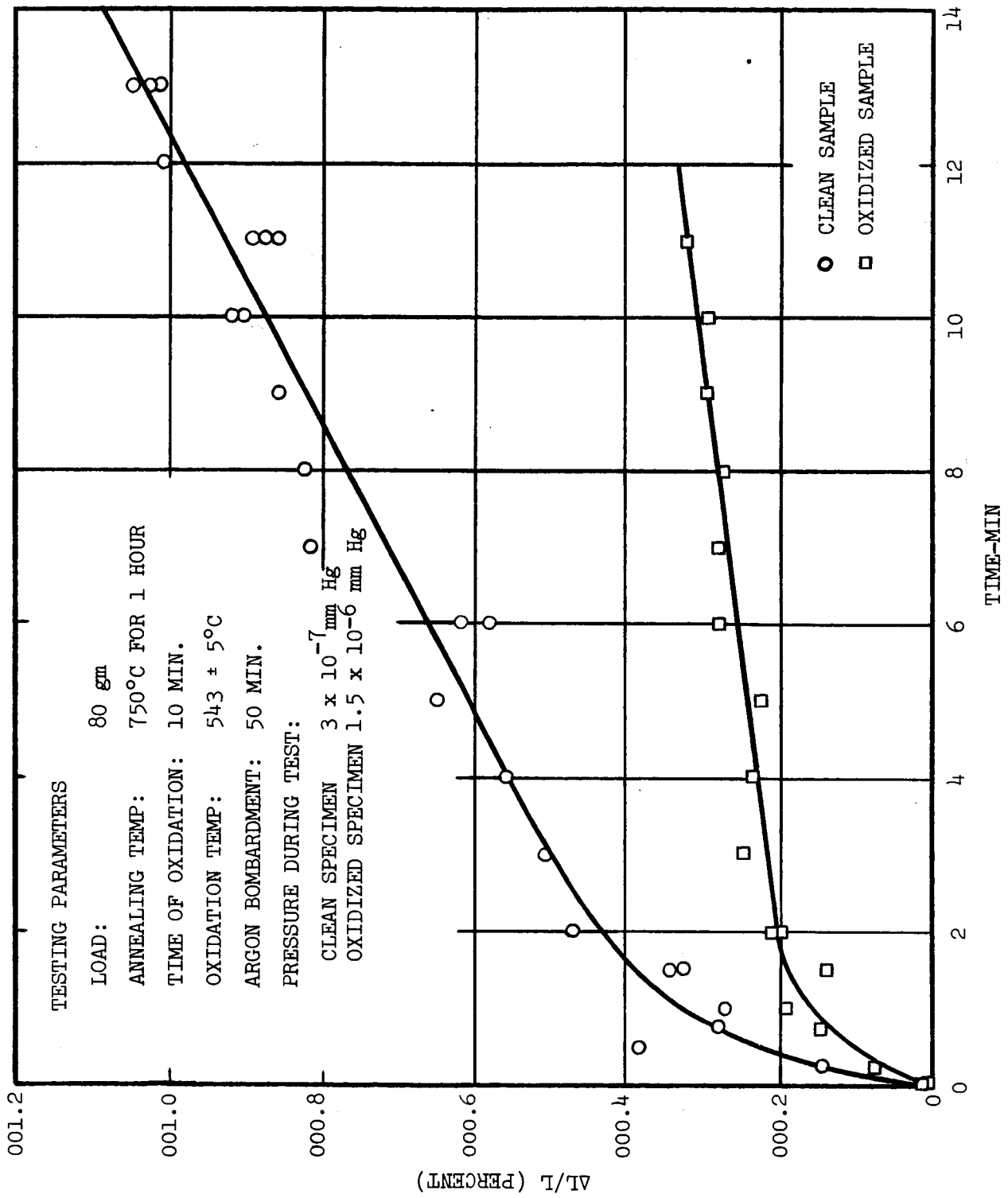


FIGURE 5 CREEP TEST OF 0.01 INCH AG WIRE OF 99.999 PERCENT PURITY

NSG-619
Supreme 2.

APPENDIX

M.S. THESIS OF ANTHONY GIANNUZZI

(DRAFT)

6

7

ABSTRACT

A series of creep tests were performed on commercial grade and high purity copper wire in high vacuum and at elevated temperatures to determine whether or not surface preparation has an effect on the creep properties of the copper.

A specimen was "cleaned" by argon ion bombardment and tested, then oxidized and tested at the same temperature and approximately the same pressure. The results indicated that the "clean" sample has a higher creep rate than does the oxidized sample.

It is presently not possible to propose a detailed dislocation model to explain the data. However, the results may be explained in part in the following manner. The creep rate of the oxidized sample is lower than for the "clean" sample because dislocations may pile up at the oxide surface or because of oxygen diffusion to grain boundaries and to dislocations. This may produce a more brittle grain boundary, an increase of frictional forces on dislocations or the oxygen may inhibit the operation of dislocation sources.

PREFACE

High vacuum creep tests cannot be compared directly with conditions in outer space. In the space environment, the outer surface of metals is constantly being "cleaned" by bombardment from high energy photons and particles. Consequently, metal, after long exposure to the outer space environment, is atomically cleaned and remains so. On the other hand, experiments in the laboratory can at best only clean a metal for a short period of time.

We attempted in this program to determine whether or not surface preparation affected the creep properties of metals in high vacuum tests. The results of this investigation may be of some assistance in the preparation of metals and alloys for the outer space environment.

The author wishes to express his gratitude to Dr. Klaus Schroder for his guidance during this program. Thanks are also expressed to Mr. Jack McKeon who helped prepare the specimens for microscopic analysis, to Mrs. Barbara Howden who drew the figures and to Miss Helen Burr and Miss Martha Coleman who did the typing.

The author also wishes to express his gratitude to the National Aeronautics and Space Administration, Washington, D.C., for their financial support.

CONTENTS

	PAGE
PREFACE.	ii
I. INTRODUCTION	1
II. EXPERIMENTAL ARRANGEMENT AND PROCEDURE	11
Experimental Arrangement	11
Testing Procedure.	14
Micrographical Analysis.	17
III. RESULTS AND DISCUSSION	19
IV. SUMMARY AND CONCLUSIONS.	22
V. REFERENCES	23

LIST OF TABLES

TABLE		PAGE
I	CREEP-RUPTURE RESULTS FOR NICKEL IN AIR AND IN VACUUM	24
II	TOTAL PRESSURE AND PARTIAL PRESSURE OF ELEMENT IN GIVEN TESTING CONDITION.	25
III	COMPARISON OF CLEANED AND OXIDIZED SAMPLES	26

LIST OF PHOTOGRAPHS

PHOTOGRAPH		PAGE
I	FRACTURED TIP OF THREE Cu SAMPLES (99.9% PURITY). . .	27
II	FRACTURED TIP OF THREE Cu SAMPLES (99.9% PURITY). . .	27
III	FRACTURED TIP OF THREE Cu SAMPLES (99.9% PURITY). . .	27
IV	FRACTURED TIP OF A HIGH PURITY Cu SAMPLE (99.999% PURITY).	28
V	GRAIN SIZE OF AS RECEIVED 99.999% PURITY Cu SAMPLE.	28
VI	GRAIN SIZE OF 99.999% PURITY Cu SAMPLE ANNEALED AT 885°C AND TESTED AT 860°C	29
VII	GRAIN SIZE OF 99.9% PURITY Cu SAMPLE ANNEALED AT 773°C AND TESTED AT 517°C	29

LIST OF FIGURES

FIGURE		PAGE
1a	CREEP CURVE OF 2A A1 AT 400°F	30
1b	CREEP CURVE OF COMMERCIAL PURE Cu AT 400°F.	30
2	CREEP CURVES AT 1500°F AND 4000 PSI	31
3	THE EFFECT OF RATE OF SURFACE REMOVAL ON THE STRESS- STRAIN CURVES OF A1-37 (TEMPERATURE 3°C AND STRAIN RATE 10 ⁻⁵ SEC ⁻¹	31
4	THE EFFECT OF CHANGE OF SLOPE IN THE RATE OF REMOVAL ON THE SLOPE OF THE FLOW CURVE	32
5	STRESS-STRAIN CURVE FOR A COMMERCIAL PURE ALUMINUM (1100-0) DEFORMED WHILE THE SURFACE WAS REMOVED AT A RATE OF 25 x 10 ⁻⁵ IN/MIN.	32
6	EFFECT OF SURFACE REMOVAL ON THE ELIMINATION OF THE YIELD POINT IN AN ALUMINUM CRYSTAL.	33
7	DECREASE IN YIELD STRESS $\Delta\tau_{\rho}$ AFTER REMOVAL OF A SURFACE LAYER	33
8	RELATIONSHIP BETWEEN DECREASE IN INITIAL YIELD STRESS, $\Delta\tau_{\rho}$, AND SHEAR STRAIN IN A1-3-12.	34
9	RELATIONSHIP BETWEEN τ_s AND γ FOR SPECIMENS A1-3-12 AND A1-1-16	34
10	SCHEMATIC DIAGRAM OF INITIAL VACUUM SYSTEM.	35
11	CREEP TEST APPARATUS.	36
12	SAMPLE AND SAMPLE SUPPORT (SCHEMATICALLY)	37
13	SCHEMATIC DIAGRAM OF REDESIGNED VACUUM SYSTEM	38
14	SCHEMATIC DIAGRAM OF LOADING SYSTEM	39
15	SCHEMATIC DIAGRAM OF TEST SECTION	40

LIST OF FIGURES (CONTINUED)

FIGURE		PAGE
16	CREEP TEST OF 0.008 INCH Cu WIRE SPECIMEN CLEANED AND TESTED, THEN OXIDIZED AND TESTED	41
17	CREEP TEST NUMBER 2 ON HIGH PURITY COPPER.	42
18	CREEP TEST NUMBER 3 ON HIGH PURITY COPPER.	43
19	CREEP TEST NUMBER 4 ON HIGH PURITY COPPER.	44
20	CREEP TEST NUMBER 6 ON HIGH PURITY COPPER.	45
21	CREEP TEST NUMBER 7 ON HIGH PURITY COPPER.	46
22	CREEP TEST OF 0.008 INCH Cu WIRE OF 99.9 PERCENT PURITY	47
23	CREEP TEST OF 0.008 INCH Cu WIRE OF 99.9 PERCENT PURITY	48

I. INTRODUCTION

In recent years, an increasing number of experiments have been conducted in order to determine the effect of surface films on the mechanical properties of metals. Investigators have demonstrated that the surface played an important part on the mechanical properties of metals. Several mechanisms such as the interaction of dislocations with a free surface, dislocations pile ups on oxide films, a "debris layer" concept, dislocation sinks and sources at the surface have been proposed to explain these experimental results.

One of the earlier investigations on the effect of surfaces on the creep properties of Al and Cu was conducted by E. D. Sweetland and E. R. Parker (1). They placed the specimens in an inert atmosphere furnace (Helium) and mechanically removed the surface layer by means of a stripping die. They applied a load to the sample and when the sample was creeping in the steady region, air was admitted. The results are given in Figure 1.

The decrease in creep rate in the air environment was as follows:

Run I Al decreased 58.3%

Run II Al decreased 18.7%

Run III Cu decreased 37.5%

Sweetland and Parker suggested several possible explanations for the phenomenon:

- 1) The oxide film can assume a higher portion of the tensile load.

They discounted this possibility because the oxide itself as deposited on the surface is imperfect, consequently it is quite unlikely that this film could assume a major portion of the tensile load.

- 2) The oxide forms a protective layer which may inhibit the formation or growth of dislocations on the surface. This means that the surface dislocation sources are pinned.
- 3) The oxide may tend to restrain the escape of dislocations at the surface.

Another investigation on the creep properties of metals was carried on by P. Shahinian and M. R. Achter (2) in their study of nickel. The creep test was carried out in vacuum (at a pressure of 2×10^{-5} mm. Hg or lower) and in air. They found a peculiarity in the creep behavior of nickel. At very low stresses the specimens tested in air had longer rupture lives and lower minimum creep rates than those tested in vacuum while at high stresses the reverse behavior was true.

The results of this investigation are presented in Table I.

The authors proposed that the creep mechanism involved two competing processes.

One process was that of oxidation strengthening in the following ways:

- 1) The surface oxide layer acts as a barrier to dislocations.
- 2) Internal oxidation strengthens the material and reduces the creep rate.

3) The oxidation process may reduce the rate of crack propagation by blunting the crack tip, thus reducing the stress concentration at the tip of the crack.

Since the last two mechanisms involved oxidation and diffusion, the authors proposed that high creep rates might reduce the diffusion effect and that the competing process, one in which the surface energy of a clean surface was reduced by oxidation, thus facilitating the propagation of a crack, may become the controlling process.

However, one may be able to consider the system in a slightly different manner. After the stress was applied, both the oxide layer and matrix material were in tension. Since the oxide was more brittle than the matrix material, it would tend to crack at stresses which would cause the matrix material to flow plastically. The crack formed is a stress raiser. This may initiate necking of the matrix, which could lead to failure.

Shahinian and Achter found that in coarse grained crystals, even at high creep rates, the air creep tested samples had a lower creep rate during the initial stages of flow as can be seen in Figure 2. However, when the stress was so high that the oxide layer cracked, the rate of oxidation at the crack tip was not great enough to blunt the tip and the crack reached a critical size and fractured the specimen.

If one again were to refer to Table I, it can be seen that in every case the reduction in area for the air tested samples was lower than for the vacuum tested samples. This supported the hypothesis that

the air tested samples fractured in a more brittle manner than did the vacuum tested samples.

Kramer and Demer (3) found that the effect of surface removal played an important part in the flow characteristics of aluminum single crystals.

They prepared five sets of crystals by a modified Bridgman technique that were capable of yielding thirty-five crystals of the same orientation.

The specimens were tested in a polishing bath so that the surface could be removed continuously as the test proceeded. The effect of the rate of surface removal on the flow characteristics of aluminum are given in Figure 3.

It can be seen from the figure that ϵ_1 and ϵ_2 (the strains at which stage I and stage II were terminated) increased as the rate of metal removed (R) was increased. The slopes of stages I and II (θ_1 and θ_2 respectively) correspondingly decreased.

However, the stresses τ_1 and τ_2 at which stages I and II ended did not change.

Since it was demonstrated that the slopes of stages I and II could be influenced by the rate at which the metal was removed from the surface, it was of interest to determine the degree to which the work hardening coefficient was reversible. The results are presented in Figure 4. These results indicate that the work hardening coefficient is completely reversible in all stages of flow.

However, another peculiarity was observed. If the rate of surface removal was increased from a low value to a high value, a large drop in load was observed. This rapid decrease in load seemed to be associated with a dislocation "pop out" phenomenon which was explained in the following manner. During deformation only a certain number of dislocations left the crystal and a number of dislocations remained in piled up arrays at the surface. When the current density was increased, the surface energy was decreased, especially at piled up sites, and the dislocations ran out in an avalanche which caused a sudden elongation of the specimen. However, interpretation of data obtained in tests on samples in electrolytes should be treated with caution. The interaction of the liquid with the metal can be quite complex, as corrosion research has shown.

Kramer (4) continued this work with a series of tensile tests on gold crystals, since it is generally believed that gold does not support a significant oxide film. He observed that when the rate of surface removal was greatly increased, there was no "pop out" effect.

However, tests on zinc single crystals (in which slip occurs primarily on the basal plane) indicated that the rate of surface removal had a pronounced effect on the flow characteristics. The "pop out" was again observed.

A three point bend test was employed to determine the effect of surface removal on the plastic flow characteristics of commercial aluminum alloys. A drop in load similar to that observed in aluminum

single crystals was seen to occur when both sides of the specimen were allowed to be removed. However, when only the compression side was removed, no drop in load was observed. It appeared again when the tension side was exposed to the polishing action.

A stress strain curve for commercially pure aluminum gave results as shown in Figure 5. When the rate of surface removal was increased from $R = 0$ to $R = 25 \times 10^{-5}$ in/min, the work hardening coefficient was decreased considerably. However, when the rate of removal was reduced to zero, the work hardening coefficient immediately returned to its initial value.

Kramer further investigated the yield point phenomenon which appears in gold and aluminum when reloaded after a given amount of prior plastic strain. This behavior was observed (as shown in Figure 6) when the specimen was unloaded and then reloaded without a surface treatment. If, however, the surface was removed after the specimen was unloaded, the yield point failed to appear.

Since it appeared that a higher density of dislocations existed at the surface than in the interior, Kramer proposed the theory of a "debris" layer existing at the surface and extending into the interior of the metal. Such a debris layer is produced near the surface of a metal by a pile up and entanglement of dislocations

There had been a question as to whether the surface effects pin dislocation sources or whether the dislocations were generated in the interior and piled up at the surfaces.

Kramer (4) attempted to resolve this question by considering the nature and spacing of slip bands deformed with or without surface removal.

He proposed that if surface sources were the dominating factor, the slip bands of the specimen deformed during polishing would be more closely spaced and narrower because active surface sources would be removed by the polishing and new sources would be generated continuously.

On the other hand, if the escape of dislocations was being altered the opposite results were to be expected. Since internal sources could operate for a longer time if dislocations could move out of the crystal (since a lower back stress is produced), he reasoned that a smaller number of sources would be necessary to produce the same amount of strain.

The experimental evidence indicated that the slip bands were more widely spaced and broader for specimens pulled with surface removal, thus indicating that the egress of dislocations from the surface was being affected.

Kramer (5) then attempted to determine the critical amount of surface that would have to be removed from aluminum single crystals.

In this series of tests, he strained the samples, removed the load and polished away the surface. Then the load was reapplied. The results are shown in Figure 7. The term $\Delta\tau_p$ was the difference between the final flow stress before the specimen was unloaded and the initial flow stress after the specimen was reloaded. The parameter Δx was one-half the total reduction in thickness after polishing. A graph of $\Delta\tau_p$ versus Δx is given in Figure 8 for various prior strains.

It can be seen from Figure 8 that $\Delta\tau_p$ does not increase with increased surface removal above a value of $\Delta x = 0.0025$ inches. He designated this value as Δx^∞ . These results indicated that $\Delta\tau^\infty = -\tau_s$ which is the stress field due to the surface layer.

The graph in Figure 9 gives a plot of τ_s versus the shear strain γ for two aluminum single crystals of different crystallographic orientations.

It was seen that the slope of stage I was a function of the orientation of the specimen axis but the slopes of stages II and III did not change markedly with orientation.

Kramer (5) proposed that the effective stress acting on a dislocation (τ) was a function not only of the applied stress τ_a and the internal stresses τ_i but also was a function of τ_s , the surface back stress caused by the debris layer.

So that

$$\tau = \tau_a - \tau_i - \tau_s$$

Kramer along with S. E. Podlaseck and H. Shen (6) in investigations of the effect of surfaces on the tensile and creep properties of aluminum in vacuum, discovered that the vacuum environment had a similar effect in reducing the work hardening and increasing creep rates as did the technique of polishing to remove the surface.

They argued that when a specimen is plastically deformed in vacuum, the rate of oxidation on the slip step is decreased. Therefore, the resistance of the oxide to the egress of dislocations is lower in vacuum than in air. As a result, the escape of dislocations is enhanced and the number of dislocations accumulated on the surface layer is reduced. This allows the stress field in the debris layer to be kept relatively low during a test in vacuum.

In a discussion of the fatigue properties of polycrystalline aluminum, Kramer, Podlaseck and Shen (7) found that the fatigue life in vacuum was greater than in air. A similar observation was made by K. U. Snowden and J. M. Greenwood (8) on the fatigue behavior of lead.

Kramer and his associates proposed that this phenomenon could be explained by the "debris layer" concept.

According to this theory, the concentration and rate of accumulation of dislocations in the surface region would be higher in air where the oxide strengthened the metal. In this case, formation of

voids and cavity dislocations would be enhanced because of the interaction of the dislocations.

However, at low pressures, the oxidation on newly created surfaces would be much lower than in air. The absence of an effective oxide barrier would permit the dislocations to escape from the surface so that the rate of accumulation of dislocation tangles in the surface region per cycle would be reduced.

Then the probability of the formation of cavity dislocations as well as the process of continual linkage of voids would be reduced.

Also, without a high rate of accumulation of dislocations, plastic relaxation would be enhanced around the freshly formed crack tip. Thus the macrocracks would grow and propagate more slowly.

Microscopic investigations of the fatigued specimens by Kramer (7) and his associates and by Snowden and Greenwood (8) indicated that many macrocracks were found in the vacuum tested specimens but none reached critical size. The investigations also indicated that the surface deformation was greater in the vacuum tested specimens. These investigations supported the "debris layer" theory as related to voids and cavity dislocations in the fatigue process.

II. EXPERIMENTAL ARRANGEMENT AND PROCEDURE

Experimental Arrangement

A schematic diagram of the initial vacuum system is given in Figure 10. A Welch Duo Seal mechanical roughing pump was connected in series with a CVC Type GF-20 oil diffusion pump, Kontes cold trap I, the Kontes 3-stage mercury diffusion pump, a second cold trap II, a large glass valve I, a third cold trap III and the Granville-Phillips ultra high vacuum valve. The Granville-Phillips valve, a Vac-Ion pump, electrical feed throughs and a high vacuum pressure gauge were connected either directly to the test section, or by means of Varian conflat flanges to the Varian Cross Connection. A bottle of high purity argon (10 ppm) was connected to the vacuum system via two glass valves to be used for ion bombardment of the sample.

A minimum pressure of 2×10^{-9} mm Hg was reached in this system at room temperature after "bake-out".

Figure 11 gives a schematic drawing of the creep test apparatus. The specimen, the heater section and the load were connected with nichrome or tantalum wires to the specimen assembly holder A in the Varian crosspiece. Initially, the load was connected via the load wire C, which bypassed the hot zone of the heater section, to hook B¹ of the nichrome specimen support wire B. The load was a high purity

iron rod, about 4" long. Loads of 400 gm, 150 gm and 185 gm were used. The specimen and heater sections were attached to the hook B'. During testing, the load was released from the load support wire C by means of a solenoid, and attached to the specimen. The specimen heater had a resistance of a few ohms and temperatures of up to 800°C could be obtained.

Although single crystals were prepared for testing, there was some difficulty in polishing them uniformly to a suitable diameter. Consequently, all data reported has been gathered from experiments on polycrystalline samples.

In creep experiments performed with the vacuum system described, commercial grade polycrystalline wire with a 0.008" diameter was used. Figure 12 shows schematically the specimen and insulating tubes which prevented electrical contact between the specimen and the high potential Mo shield. The Cu wire was looped over each end of the nichrome wire support A and A'. The nichrome wire A extended from the top of the sample to point B and nichrome wire A' from the lower end of the sample to point B'. The tips of the nichrome wire, B and B' were photographed. Their distance on the film was measured on the microscopic stage of a metallograph.

A silica tube was slipped over the top detection wire and positioned at point C in order to insulate the specimen from the nichrome

wire. A thermocouple was inserted through the ceramic tube D and mechanically connected to the nichrome wire.

A schematic diagram of the redesigned vacuum system is given in Figure 13. In this system, a Welch-Duo-Seal mechanical pump was connected in series with a NRC Type 149 metal diffusion pump (pumping speed 60 L/second), a Kontes glass valve, a Kontes cold trap, a 1" Granville-Phillips ultra high vacuum valve and two Varian Cross connections to the test cell. In addition, a Vac-Ion pump, a Varian Titanium Sublimation pump (pumping speed 50 L/second) and a Red Head Ultra High Vacuum Gauge (or a Partial Pressure Gauge) were connected to the ultra high vacuum section by the flanges of the Varian Cross connections. The two vacuum gauges placed as shown, and the Vac-Ion pump gave an accurate measure of the pressure in the vacuum system. A flexible bellows section was used to apply and release the load. Figure 14 shows schematically the bellows section. The load, which rested on the lever support, could be lowered or raised by moving the bellows in the appropriate direction. In this manner the load could easily be applied to or released from the sample.

A diagram of the redesigned test section is given in Figure 15. The section consisted of a tantalum heater coil with three molybdenum radiation shields. This section was supported by a stainless steel tube. The sample was looped around two nichrome wires as described previously and placed in position in the test section. The thermo-

couple was placed through two of the six silica tubes used to insulate the molybdenum radiation shields from the heater element and suspended inside the heater section. A flexible electrical connection was made from the sample to one of the other terminals of the 8-lead electrical feedthrough. This lead was used for argon bombarding. A negative potential was applied to the sample, the positive terminal being ground. The load was then connected between the lower nichrome wire hook and the lever support arm. Measurement of the elongation of the sample was made by photographing the relative displacement of the nichrome wires. The load used for these tests was 42.5 gm., and the testing temperature ranged from 700°C to 850°C. The samples used were either the commercial grade 0.008" copper wire or the 99.999% high purity 0.010" copper wire.

Testing Procedure

The testing procedure was the same for both vacuum setups. The mechanical pump was turned on and the entire system was pumped down to about 10^{-1} Torr. Then the oil diffusion pump was activated to reduce the pressure to about 10^{-5} Torr. The sample was then annealed for about two hours at a temperature which was above the testing temperature. In some of the tests the system was "baked out" to reduce the pressure. However, the "bake out" process did not have a significant effect in reducing the pressure during which time the

experiment was being conducted so that it was generally not performed. After annealing the sample was allowed to cool to room temperature. Argon was introduced and the system was flushed. After three flushings, and when the pressure was again reduced to about 10^{-5} Torr, argon was introduced into the test section to raise it to a pressure of 10^{-1} to 10^{-2} Torr and the Granville-Phillips valve was closed. Activation of the Titanium Sublimation pump should remove only contaminants but no argon from the system. The specimen was then "cleaned" by bombardment with argon ions for about 40 to 90 minutes. The potential difference between anode and cathode was about 700 volts and the ion current density was estimated to be of the order of 0.5 mA/cm^2 . After argon bombarding, the system was evacuated to a pressure of about 10^{-5} Torr by means of the diffusion pump. Then, the metal valve was closed, and a pressure of less than 10^{-7} Torr was obtained by the Vac-Ion pump and the Titanium Sublimation pump. The heater element was activated immediately and the sample reached its equilibrium test temperature within 20 to 30 minutes. This time interval and the temperature should have been long enough for the sample to recover from defects produced by the ion bombardment. The temperature variation during the test was never greater than $\pm 10^\circ\text{C}$. The test pressure was always 2×10^{-5} Torr or lower.

When the sample reached the equilibrium temperature, the load was applied and the specimen length change was recorded photographi-

cally. After about 20 photographs (recorded in 1/4, 1/2 and 1 minute intervals), the sample was unloaded, air was introduced into the system and the sample was oxidized. The heater current remained constant; however, heat loss due to conduction and convection, in air reduced the oxidation temperature well below the testing temperature.

After oxidation (which was performed in a time interval of from 8 minutes to 1 hour) the pressure was again reduced to about the same level as the first part of the creep test. The load was reapplied; and the length change was again recorded. The entire testing time was usually about 30 minutes or less.

A series of partial pressure measurements were made to determine the pressure of the component gases in the system. The head of the gauge was placed just above the test section in the testing chamber (see Figure 13).

The results are given in Table II for the following test conditions:

- 1) Mechanical and oil diffusion pump operating; sample at room temperature.
- 2) Mechanical and oil diffusion pump operating; sample annealed for 1-1/2 hours at 800°C, sample at annealing temperature.
- 3) Mechanical and oil diffusion pump operating after anneal; sample cooled to room temperature.

- 4) Mechanical and oil diffusion pump operating after anneal, sample at room temperature, liquid nitrogen in dewar surrounding Ti pump.
- 5) Mechanical and oil diffusion pump operating after anneal, sample at room temperature, liquid nitrogen in dewar surrounding Ti pump, Titanium Sublimation pump operating.
- 6) Mechanical and oil diffusion pump operating after anneal, sample at room temperature, liquid nitrogen in dewar surrounding Ti pump after Ti pumping concluded.
- 7) Vac-Ion pump operating, no liquid nitrogen in dewar.
- 8) Mechanical and oil diffusion pump operating; sample has been Argon bombarded.
- 9) Vac-Ion pump also operating, cleaned sample at test temperature.
- 10) Sample at test temperature after oxidation for 10 minutes, Vac-Ion pump, mechanical pump and oil diffusion pump operating.

Micrographical Analysis

In order to reveal the substructure of the specimens, some of the samples were analyzed microscopically. The fractured surface of the samples was photographed at a magnification of 50X, then the samples were mounted, mechanically polished and etched in an attempt

to determine the grain size of the specimens and also to determine whether or not slip lines could be observed.

Photographs I through IV give the fracture surface of some of the samples tested. Photographs I through III are of 0.008", 99.9% pure Cu which were all annealed at $\sim 750^{\circ}\text{C}$ and tested at between 450°C and 550°C . Photograph IV is of a 99.999% pure Cu sample annealed at 885°C and tested at 860°C . One can see parts of the quite brittle oxide coating on the surface of this sample.

The grain size of the samples in the as received condition and in the annealed condition is given in Photographs V through VII. Although the grain size of the 99.999% pure sample, Photograph VI, (annealed and tested at 800°C or above) is large, no single grain is as large as the diameter of the sample. This may explain why no slip lines were observed. These samples were photographed at a magnification of 200X.

III. RESULTS AND DISCUSSION

Although the bulk of the experiments were performed on high purity copper wire (99.999% Cu) with a nominal diameter of 0.01", several preliminary tests were performed on the commercial grade 0.008" copper wire using the initial vacuum setup. A load of 400 gm. was applied to the samples at a temperature of approximately 405°C. During these tests, the creep rate was so low that the length change was smaller than the experimental error (<0.1%). However, the same sample fractured immediately after oxidation.

In order to obtain a creep curve for the "cleaned" and oxidized sample, an experiment was conducted at a slightly higher temperature (465°C) with a smaller load (185 gm). The creep curve for this sample (specimen 1) is given in Figure 16 and the results are listed in Table III.

A series of experiments were performed in the redesigned vacuum system on high purity copper wire (99.999% Cu) with a diameter of 0.01". The experimental results are listed in Table III and in Figures 17 to 21. Also listed in Table III are results on copper of 99.9% purity with a nominal diameter of 0.008" (9). Figures 22 and 23 give creep curves for these specimens. The tests on high purity copper were performed so that the creep rates of the "cleaned" and oxidized samples could be obtained at higher tempera-

tures. This testing procedure would also insure that the vapor pressure of the sample was close to the testing pressure of the system.

The measurements made on high purity copper wire and the results of the tests on 99.9% pure Cu confirmed the preliminary results obtained on commercial grade copper. These results indicated that the creep rate of samples tested in high vacuum decreased markedly after oxidation.

One of the experimental difficulties associated with a high vacuum test is that a direct comparison between results obtained from different specimens is not always possible. For instance, the temperature measurement may be inaccurate if one replaces the sample because the position of the thermocouple may change. However, the variation of creep rate (before and after oxidation) on one sample should be a reliable indicator of changes of the sample because the testing conditions remain the same.

G. Gorsha (9) has performed a series of experiments on silver under the same general experimental conditions. His results indicated the same basic creep behavior as the results on copper. However, at the test pressure and temperature during which his tests were conducted, silver does not oxidize. These results indicate that the "debris layer" concept by Kramer may not explain all experiments. There may be a number of mechanisms responsible for

the creep behavior of the specimens. When a load is applied to a specimen after severe oxidation, dislocations pile up at the surface because of the oxide film. This pile up of dislocations exerts a back stress which may render the dislocation source inactive. This effect will result in a strengthening of the material and consequently a lower creep rate.

However, the oxide surface of copper is more brittle than the matrix. At a sufficiently high stress, the oxide may crack resulting in a stress raiser at the tip of the crack. The matrix material in the vicinity of the crack tip will flow in order to relieve the stress. Thus, the sample may neck down and fail at that point.

Severe oxidation may also strengthen the copper by diffusing into the material. This diffusion will have two effects. The oxygen may diffuse to the grain boundaries, thus strengthening them, or it may diffuse to a dislocation and act either as a drag on the motion of the dislocation or lock a dislocation source. In either case, the resulting effect is a lower creep rate and a more brittle material.

IV. SUMMARY AND CONCLUSIONS

The experimental investigations on commercial grade and high purity polycrystalline copper wire indicated that specimens "cleaned" by ion bombardment have a higher creep rate than the same specimens when badly oxidized in air.

The effect may be explained in part by a pile up dislocation at the oxide barrier. This pile up and the back stress produced decreases the creep rate of the metal. Internal oxidation may also strengthen the material by diffusion of oxygen to grain boundaries and to dislocations. The diffusion of oxygen to grain boundaries makes intergranular slip more difficult. Since the oxide surface is more brittle than the matrix, a crack in the oxide will produce high stresses which may initiate necking of the matrix and fracture. It is, however, also possible that oxygen diffuses into the metal and either inhibits operation of dislocation sources, or increases the frictional force on moving dislocations.

However, presently it is not possible to develop a model to explain uniquely the experimental results.

V. REFERENCES

1. E. D. Sweetland and E. R. Parker, "Effect of Surface Condition on Creep of Some Commercial Metals," Journal of Applied Mechanics, Vol. 20, pp 30-32 (March, 1953).
2. P. Shahinian and M. R. Achter, "A Comparison of the Creep-Rupture Properties of Nickel in Air and in Vacuum," Transactions, Met. Soc. AIME, Vol. 215, pp 37-41 (February, 1959).
3. I. R. Kramer and L. J. Demer, "The Effect of Surface Removal on the Plastic Behavior of Aluminum Single Crystals," Transactions, Met. Soc. AIME, Vol. 221, pp 780-786 (August, 1961).
4. I. R. Kramer, "The Effect of Surface Removal on the Plastic Flow Characteristics of Metals. Part II: Size Effects, Gold, Zinc, and Polycrystalline Aluminum," Transactions, Met. Soc. AIME, Vol. 227, pp 1003-1010 (August, 1963).
5. I. R. Kramer, "Influence of the Surface Layer on the Plastic-Flow Deformation of Aluminum Single Crystals," Transactions, Met. Soc. AIME, Vol. 233, pp 1462-1466 (August, 1965).
6. H. Shen, S. E. Podlaseck, and I. R. Kramer, "Vacuum Effects on the Tensile and Creep Properties of Aluminum," Transactions, Met. Soc. AIME, Vol. 233, pp 1933-1938 (November, 1965).
7. H. Shen, S. E. Podlaseck, and I. R. Kramer, "Effect of Vacuum on the Fatigue Life of Aluminum," Acta Metallurgica, Vol. 14, pp 341-345 (March, 1966).
8. K. U. Snowden and J. Neill Greenwood, "Surface Deformation Differences between Lead Fatigued in Air and in Partial Vacuum," Transactions, Met. Soc. AIME, Vol. 212, pp 626-627 (October, 1958).
9. K. Schroder, A. Giannuzzi, and G. Gorsha, "Creep at Elevated Temperatures and High Vacuum," Semi-Annual Report No. 5 (December, 1966).

TABLE I

Creep-Rupture Results For Nickel In Air And In Vacuum

TIME °F	STRESS PSI	ATMOSPHERE	RUPTURE LIFE,HR	MINIMUM CREEP RATE PCT PER HR	ELONGATION PCT	REDUCTION OF AREA PCT
<u>Fine-Grained Material</u>						
1200	12000	Air	3.0	3.0	19	18
		Vacuum	6.2	1.9	23	24
	9000	Air	19.3	0.48	17	15
		Vacuum	29.5	0.33	19	18
	6000	Air	179.8	0.035	14	10
		Vacuum	197.4	0.030	14	12
	4500	Air	807.1	0.0072	13	8.6
		Vacuum	768.6	0.0066	12	9.4
1500	5000	Air	3.2	1.9	15	13
	4000	Air	7.3	0.83	12	10
		Vacuum	9.5	0.58	14	12
	3500	Air	20.3	0.24	10	8
	3000	Air	53.9	0.12	13	7
		Vacuum	23.5	0.18	12	8
	2500	Air*	4000.0+	0.0003	13	3
		Vacuum	48.5	0.061	8	8
	2000	Air*	3000.0+	0.0005	10	1
		Vacuum	111.8	0.025	11	7
<u>Coarse-Grained Material</u>						
1500	4000	Air	1.9	2.16	10	8
		Vacuum	2.8	1.6	12	11
	3000	Air	8.1	0.33	11	5
		Vacuum	13.5	0.33	14	9
	2500	Air	62.1	0.10	10	6
		Vacuum	19.5	0.16	9	11
	2000	Air*	3817.0+	0.0007	6	0
		Vacuum	39.5	0.041	8	7

* Unfractured Specimen.

TABLE II

Total Pressure And Partial Pressure Of Element In Given Testing Condition

ELEMENT PRESENT	TESTING CONDITION									
	1	2	3	4	5	6	7	8	9	10
TOTAL PRESSURE ¹	1.9×10^{-5}	5×10^{-5}	7.5×10^{-5}	2×10^{-5}	2.4×10^{-6}	3.1×10^{-6}	9.4×10^{-7}	1.5×10^{-5}	6.8×10^{-6}	1.2×10^{-5}
H ⁺	1.4×10^{-6}	1.8×10^{-6}	2.2×10^{-6}	7.5×10^{-7}	8.5×10^{-8}	1.7×10^{-7}	4×10^{-8}	5.6×10^{-7}	1.9×10^{-7}	6.3×10^{-7}
H ₂ ⁺	3.7×10^{-6}	1.6×10^{-5}	1.3×10^{-5}	4.7×10^{-6}	6×10^{-7}	1×10^{-6}	2.6×10^{-7}	4.5×10^{-6}	1.5×10^{-6}	5×10^{-6}
He ⁺	--	1.4×10^{-7}	9×10^{-8}	1.2×10^{-8}	--	--	--	1.1×10^{-8}	--	1.4×10^{-8}
TOTAL PRESSURE ²	1.9×10^{-5}	7×10^{-5}	8×10^{-5}	2×10^{-5}	4×10^{-6}	2.6×10^{-6}	8.2×10^{-7}	2×10^{-5}	8×10^{-6}	1.4×10^{-5}
N ₂ ⁺⁺	7.8×10^{-7}	9×10^{-7}	1.2×10^{-6}	7×10^{-7}	4.1×10^{-8}	3.6×10^{-8}	3.5×10^{-8}	7×10^{-7}	3.4×10^{-7}	5×10^{-7}
O ⁺	2.1×10^{-7}	--	--	3.7×10^{-7}	--	--	--	8×10^{-7}	--	--
OH ⁺	--	1.3×10^{-6}	1.8×10^{-6}	6.5×10^{-7}	--	--	--	5.8×10^{-7}	2.1×10^{-7}	5.8×10^{-7}
HOH ⁺	4.4×10^{-6}	2×10^{-6}	6.1×10^{-6}	5.6×10^{-7}	3.8×10^{-7}	4.1×10^{-7}	1×10^{-7}	1.9×10^{-7}	3.3×10^{-7}	1×10^{-6}
Ar ⁺⁺	--	--	--	--	--	--	--	1.9×10^{-8}	--	--
O ₂ ⁺	3.5×10^{-6}	5.1×10^{-6}	6.3×10^{-6}	4×10^{-6}	2.7×10^{-7}	3×10^{-7}	2.2×10^{-7}	5.5×10^{-6}	2×10^{-6}	2×10^{-6}
Cr ⁺ or V ⁺	1.1×10^{-7}	1×10^{-6}	7.5×10^{-7}	1.5×10^{-7}	1.4×10^{-7}	1.2×10^{-7}	4.9×10^{-8}	1.8×10^{-7}	3×10^{-7}	5×10^{-7}
Ni ⁺ or Cu ⁺ or Zn ⁺	2.1×10^{-8}	8×10^{-8}	3.3×10^{-7}	1×10^{-7}	1.4×10^{-7}	1×10^{-7}	1.8×10^{-8}	6.5×10^{-9}	9×10^{-8}	6×10^{-8}

1) Total Pressure Reading For Low Mass Range Of Partial Pressure Gauge.

2) Total Pressure Reading For High Mass Range Of Partial Pressure Gauge.

ALL PRESSURES IN TORR.

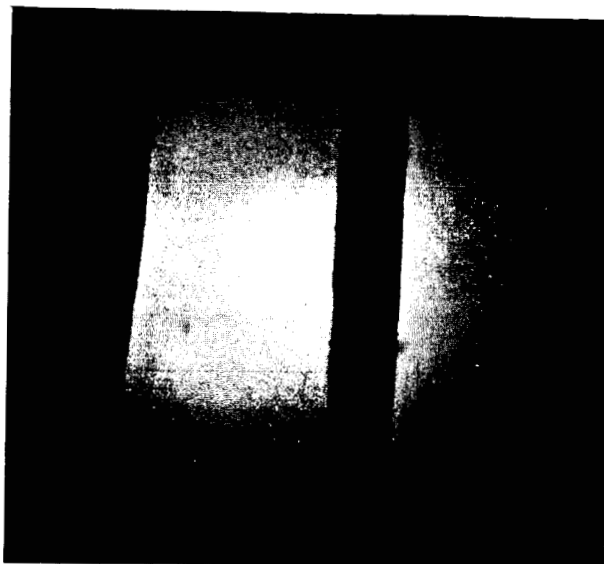
TABLE III

COMPARISON OF CLEANED AND OXIDIZED SAMPLES

SAMPLE TESTED	TEST TEMPERATURE °C	STRAIN RATE		TENSILE STRESS PSI	OXIDATION TIME MINUTES	ANNEALING TIME HOURS	ANNEALING TEMPERATURE °C	TEST PRESSURE (TORR)
		CLEAN SAMPLE	IN/IN/MIN OXIDIZED SAMPLE					
Commercial Grade Cu (1)	465°C	0.00029	0.00016	8120	45	3	600°C	1x10 ⁻⁶
	460°C			8120				5x10 ⁻⁶
High Purity Cu (2)	785°C	0.0005	0.0001	1180	15	6	800°C	9x10 ⁻⁷
	785°C			1180				8x10 ⁻⁶
High Purity Cu (3)	845°C	0.00086	0.00018	1180	8	5	885°C	7x10 ⁻⁷
	845°C			1180				5x10 ⁻⁶
High Purity Cu (4)	830°C	0.00044	0.00008	1180	10	2	850°C	8x10 ⁻⁶
	830°C			1180				5x10 ⁻⁶
High Purity Cu (5)	835°C	0.00033	Immediate Frac.	1180	10	1	860°C	4x10 ⁻⁶
	835°C			1180				1x10 ⁻⁵
High Purity Cu (6)	830°C*	0.0006	0 ⁺	1180	10	1	845°C	3x10 ⁻⁶
	830°C			1180				2x10 ⁻⁵
99.9% Pure Cu (7)	460°C	0.0012	0.00025	9950	60	1 1/2	745°C	1x10 ⁻⁶
	460°C			9950				5x10 ⁻⁶
99.9% Pure Cu (8)	475°C	0.0015	No Second Stage Creep	9950	60	1 1/2	750°C	3x10 ⁻⁶
	510°C			9950				2x10 ⁻⁴

+ Within Experimental Accuracy

* Estimated



PHOTOGRAPH I



PHOTOGRAPH II



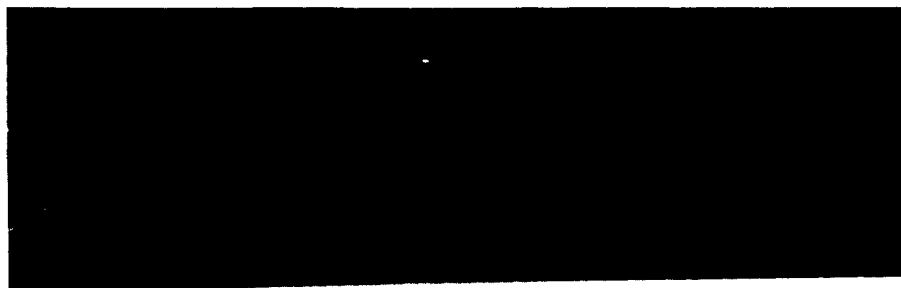
PHOTOGRAPH III

FRACTURED TIP OF THREE Cu SAMPLES (99.9% PURITY)



PHOTOGRAPH IV

FRACTURED TIP OF A HIGH PURITY Cu SAMPLE
(99.999% PURITY)



PHOTOGRAPH V

GRAIN SIZE OF AS RECEIVED 99.999% PURITY Cu SAMPLE



PHOTOGRAPH VI

GRAIN SIZE OF 99.999% PURITY Cu SAMPLE ANNEALED
AT 885°C AND TESTED AT 860°C



PHOTOGRAPH VII

GRAIN SIZE OF 99.9 % PURITY Cu SAMPLE ANNEALED AT
773°C AND TESTED AT 517°C

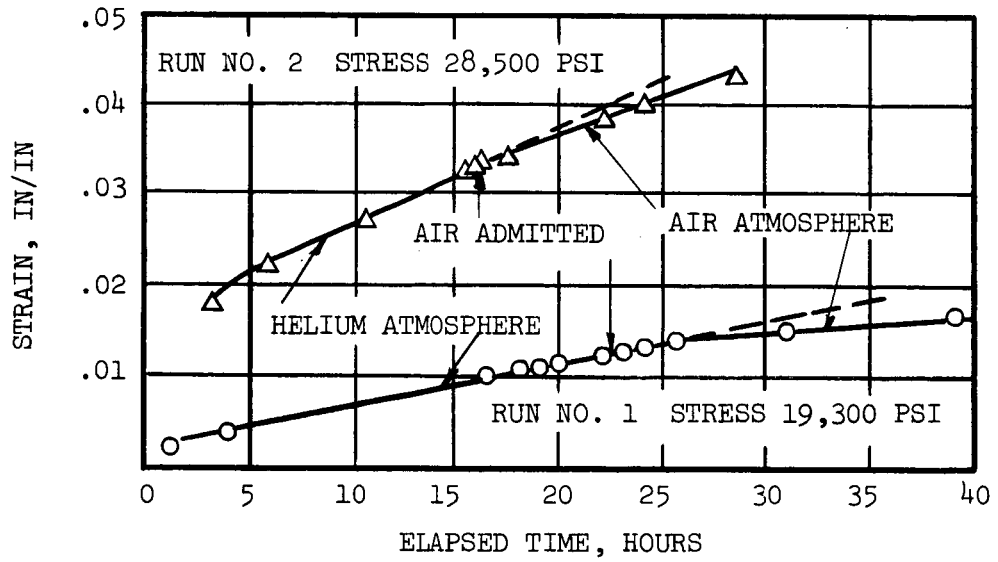


FIGURE 1a CREEP CURVE OF 2A Al AT 400°F

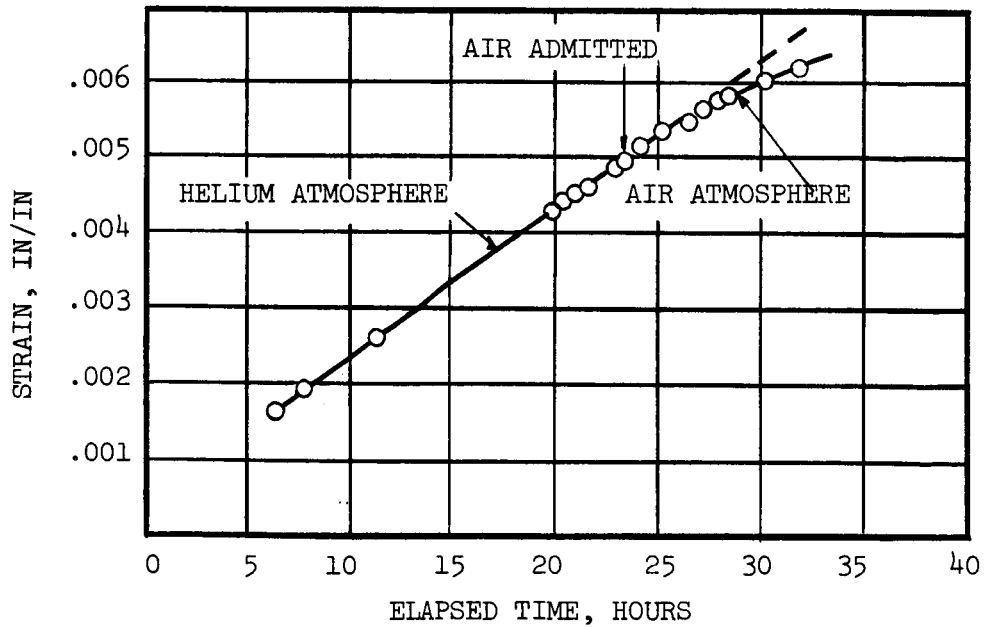


FIGURE 1b CREEP CURVE OF COMMERCIAL PURE Cu AT 400°F

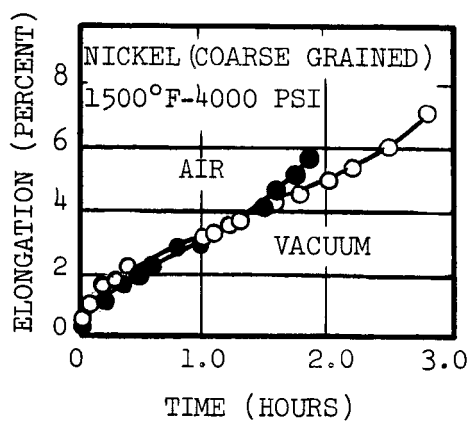


FIGURE 2 CREEP CURVES AT 1500°F AND 4000 PSI

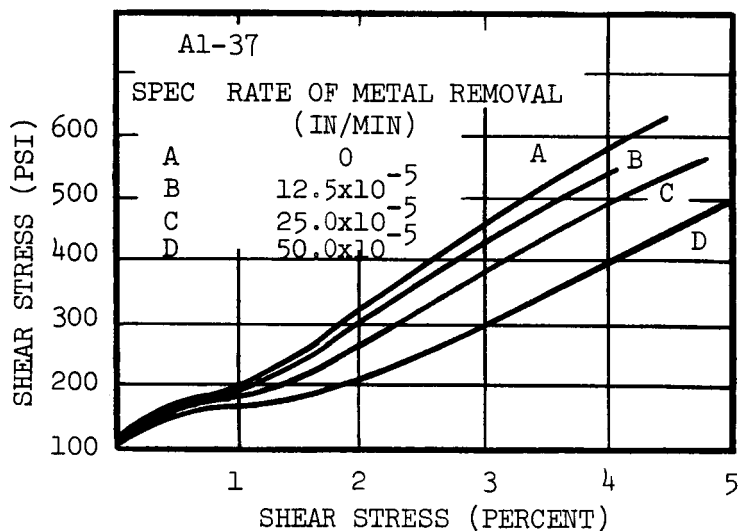


FIGURE 3 THE EFFECT OF RATE OF SURFACE REMOVAL ON THE STRESS STRAIN CURVES OF Al-37 (TEMPERATURE 3°C AND STRAIN RATE 10^{-5}SEC^{-1})

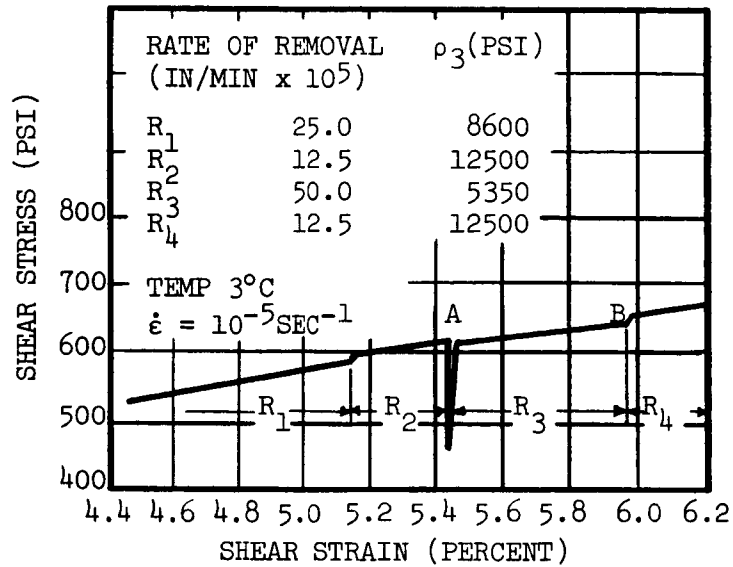


FIGURE 4 THE EFFECT OF CHANGE OF SLOPE IN THE RATE OF REMOVAL ON THE SLOPE OF THE FLOW CURVE

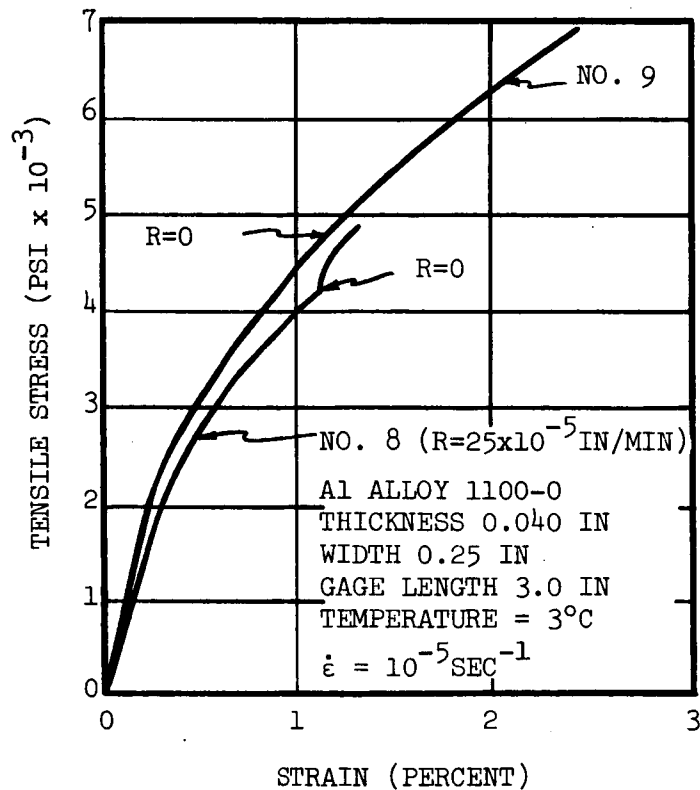


FIGURE 5 STRESS-STRAIN CURVE FOR A COMMERCIALY PURE ALUMINUM (1100.0) DEFORMED WHILE THE SURFACE WAS REMOVED AT A RATE OF 25×10^{-5} IN/MIN

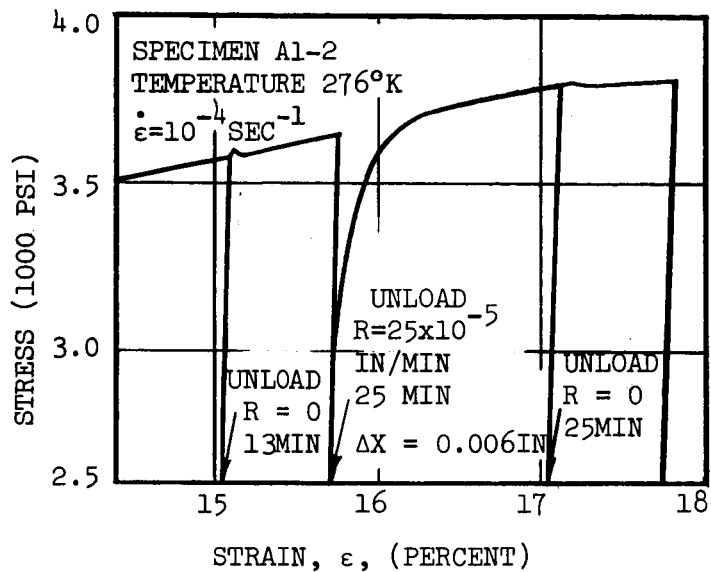


FIGURE 6 EFFECT OF SURFACE REMOVAL ON THE ELIMINATION OF THE YIELD POINT IN AN ALUMINUM CRYSTAL

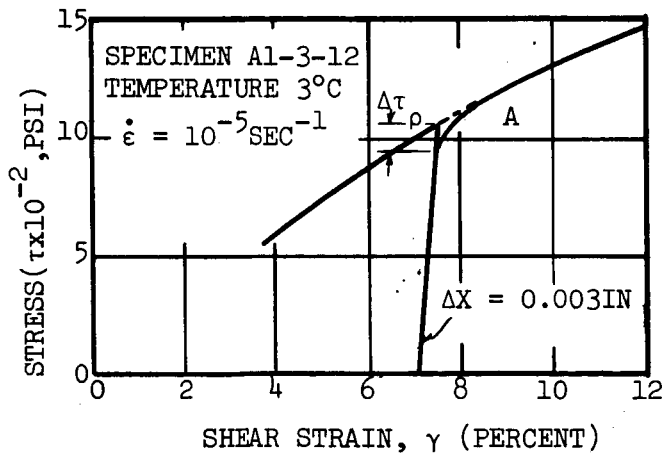


FIGURE 7 DECREASE IN YIELD STRESS $\Delta \tau$ AFTER REMOVAL OF A SURFACE ρ LAYER

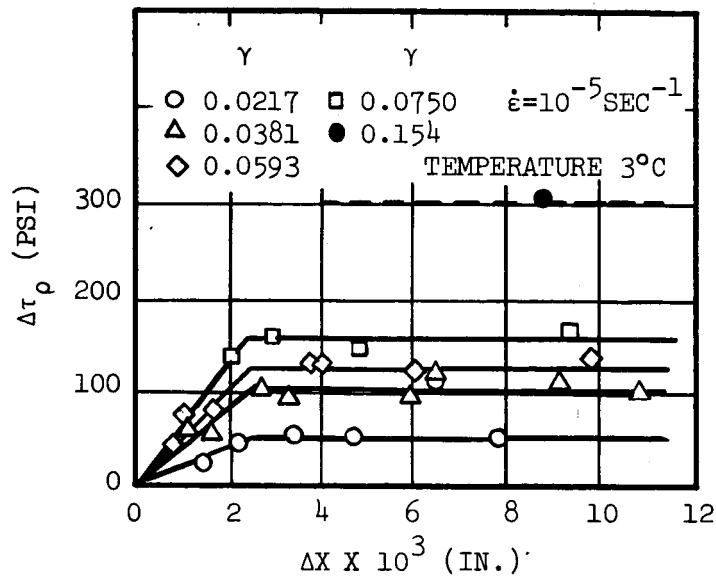


FIGURE 8 RELATIONSHIP BETWEEN DECREASE IN INITIAL YIELD STRESS, $\Delta\tau_p$ AND SHEAR STRAIN IN Al-3-12

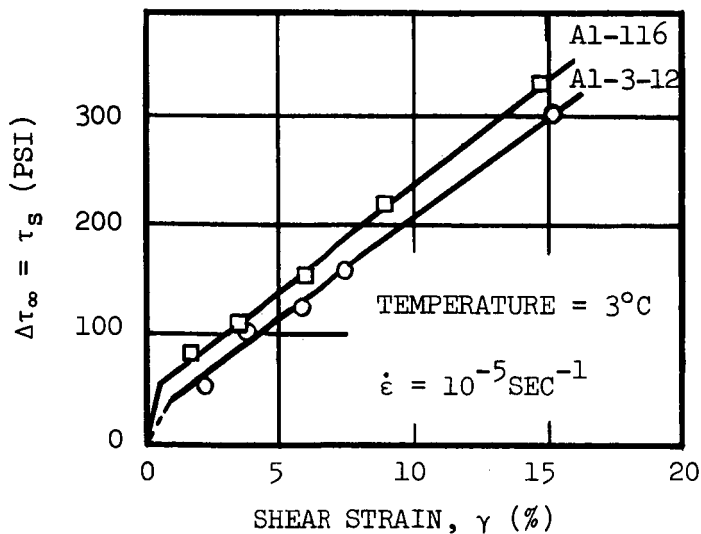


FIGURE 9 RELATIONSHIP BETWEEN τ_s AND γ FOR SPECIMENS Al-3-12 AND Al-1-16

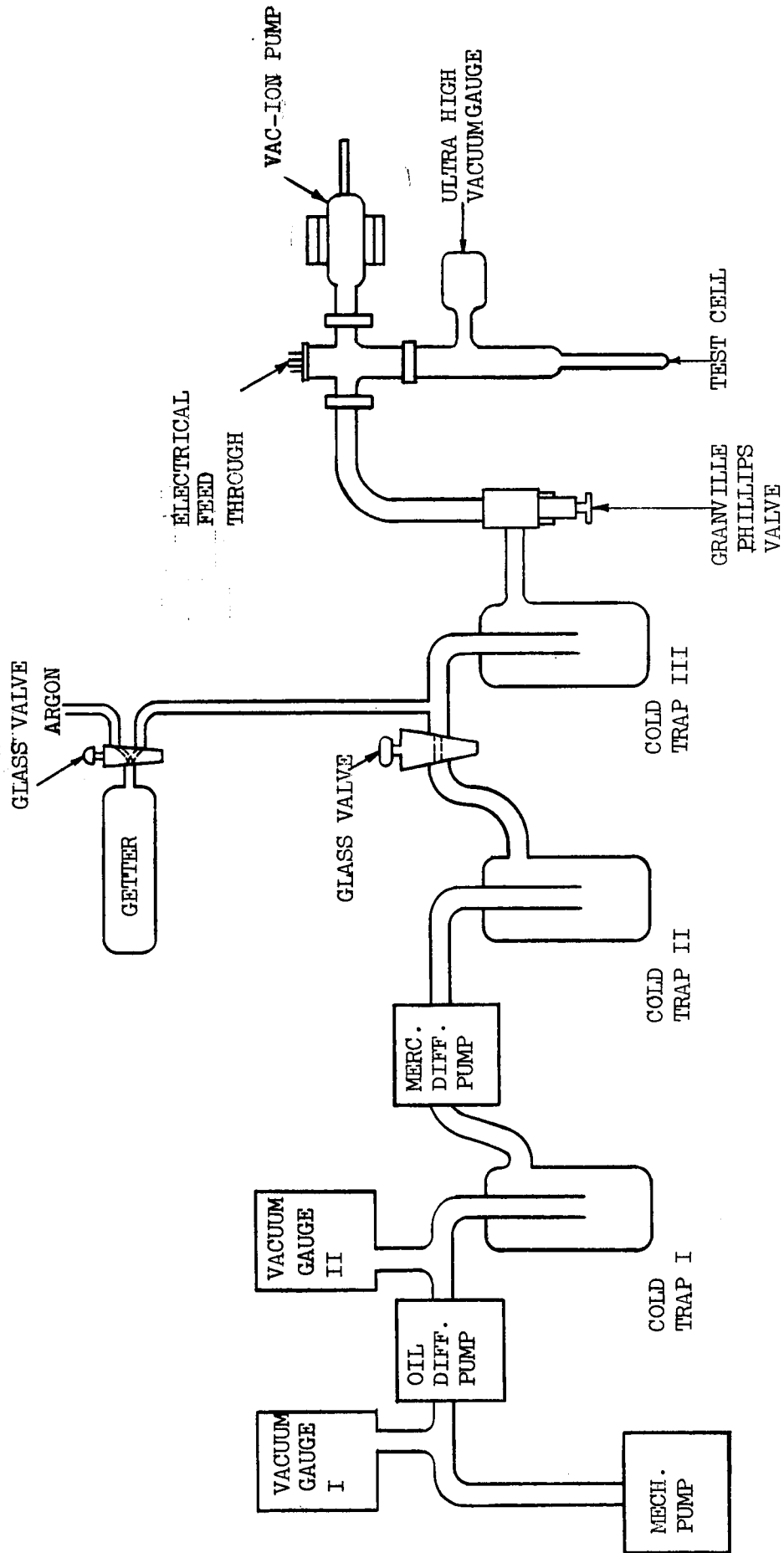


FIG. 10 SCHEMATIC DIAGRAM OF INITIAL VACUUM SYSTEM

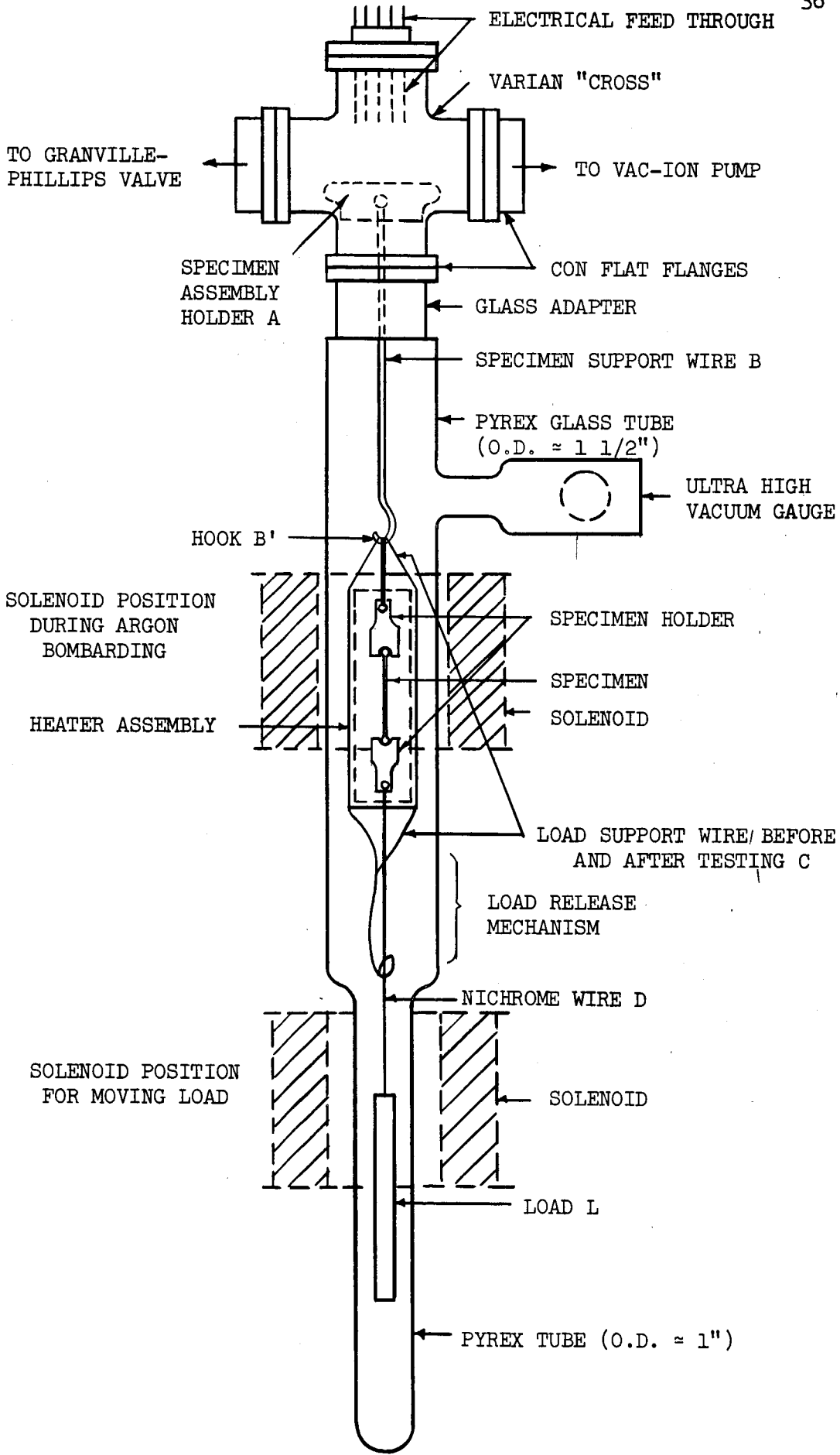


FIG. 11 CREEP TEST APPARATUS

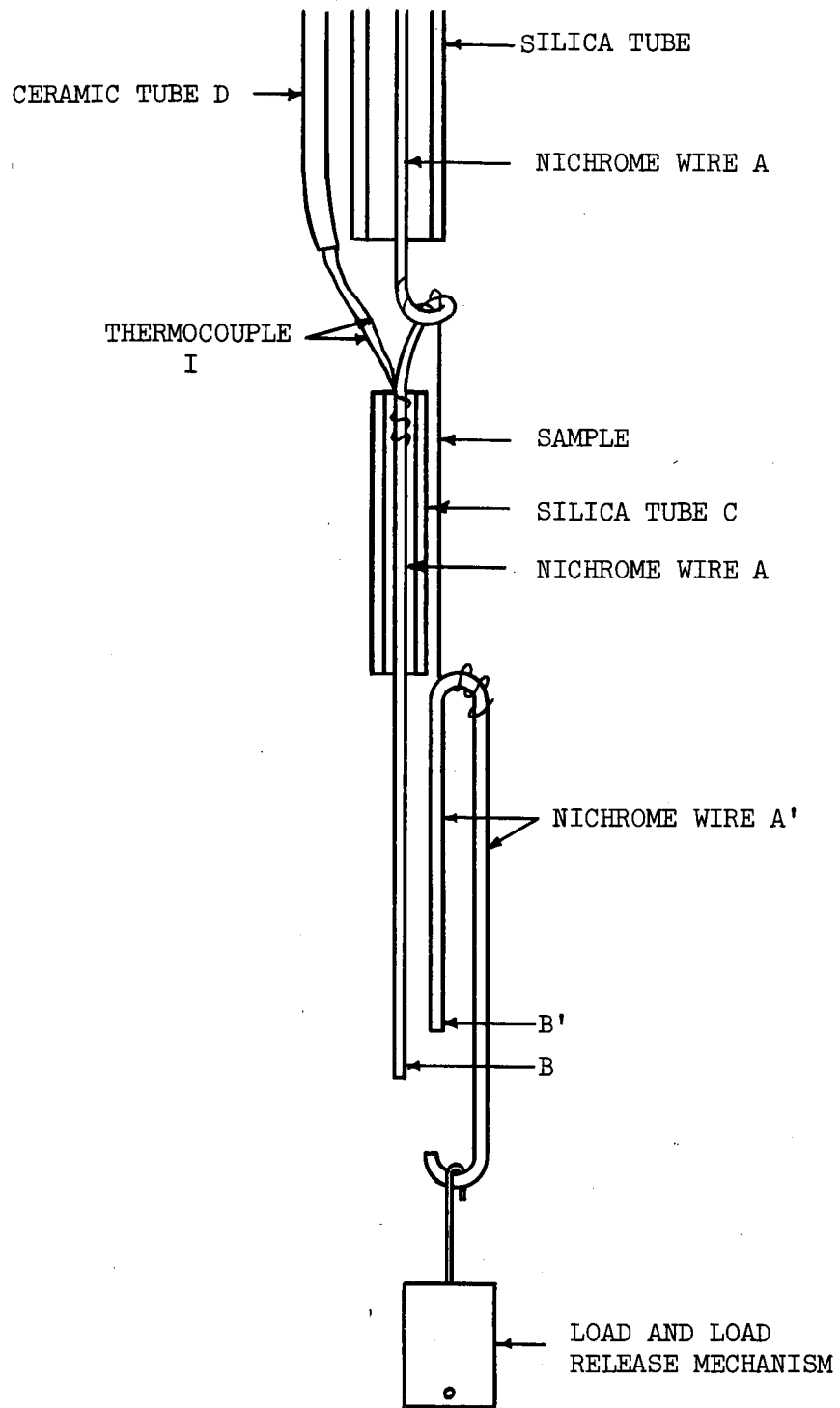


FIG. 12 SAMPLE AND SAMPLE SUPPORT (SCHEMATICALLY)

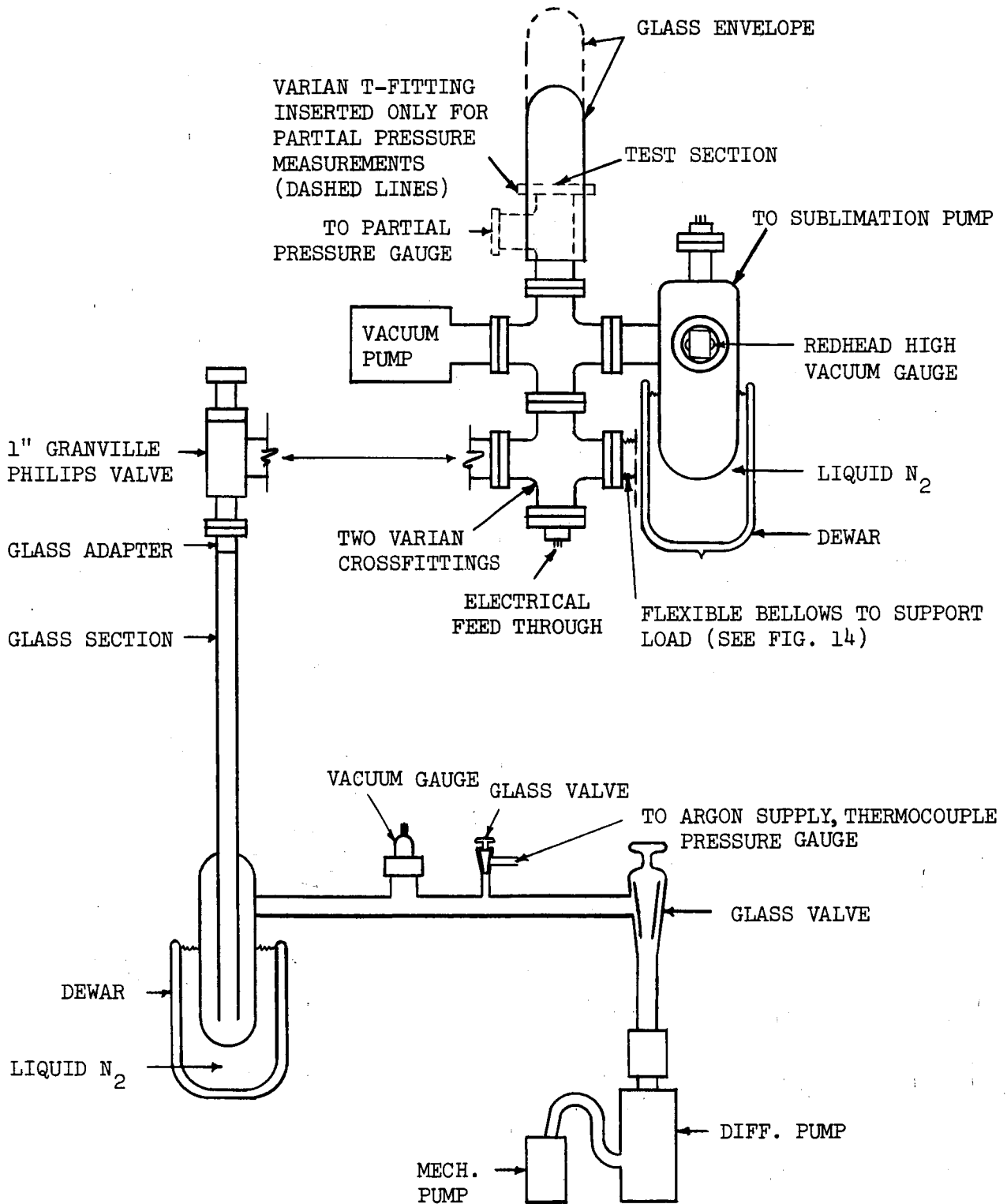


FIG. 13 SCHEMATIC DIAGRAM OF REDESIGNED VACUUM SYSTEM

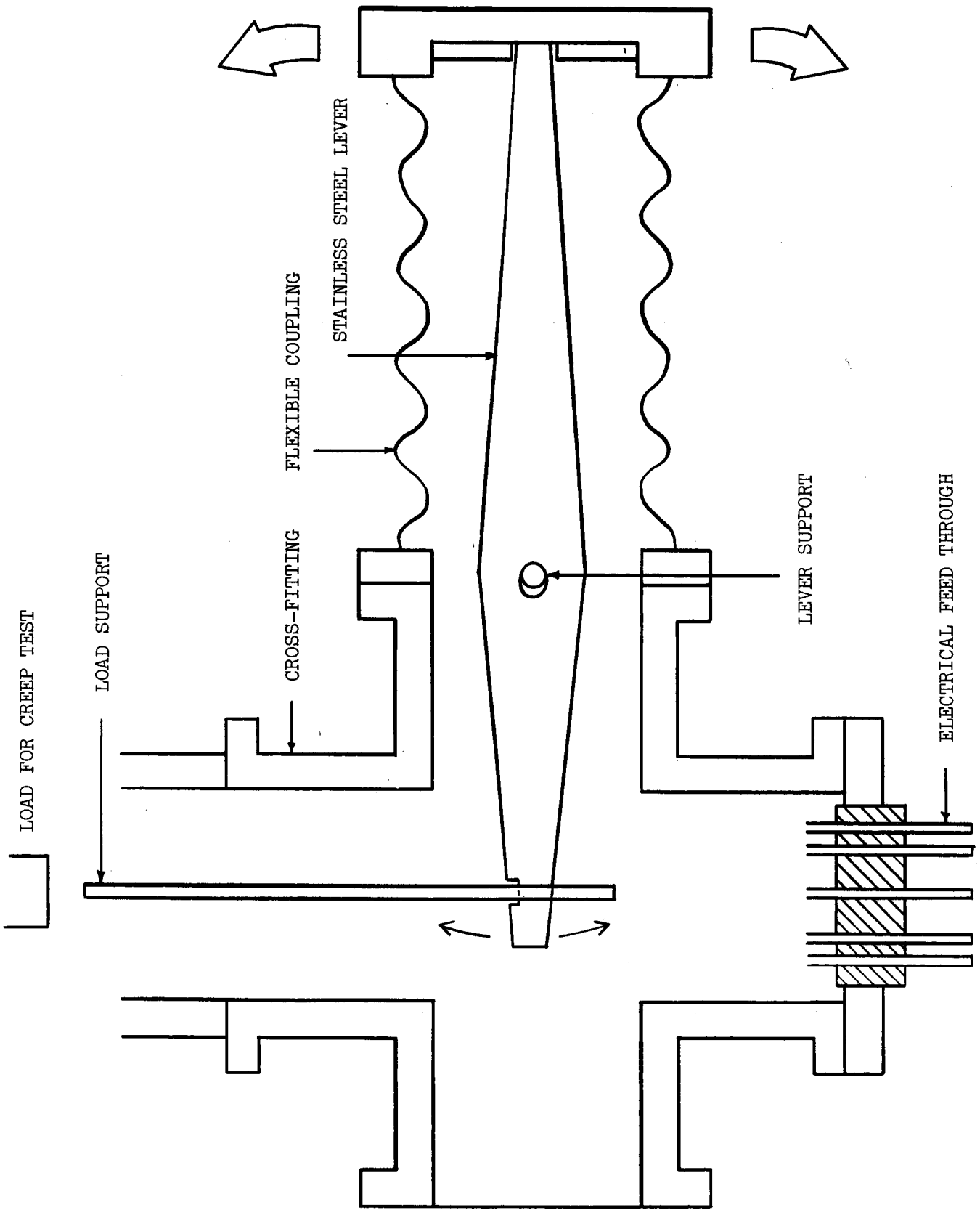


FIG. 14 SCHEMATIC DIAGRAM OF LOADING SYSTEM

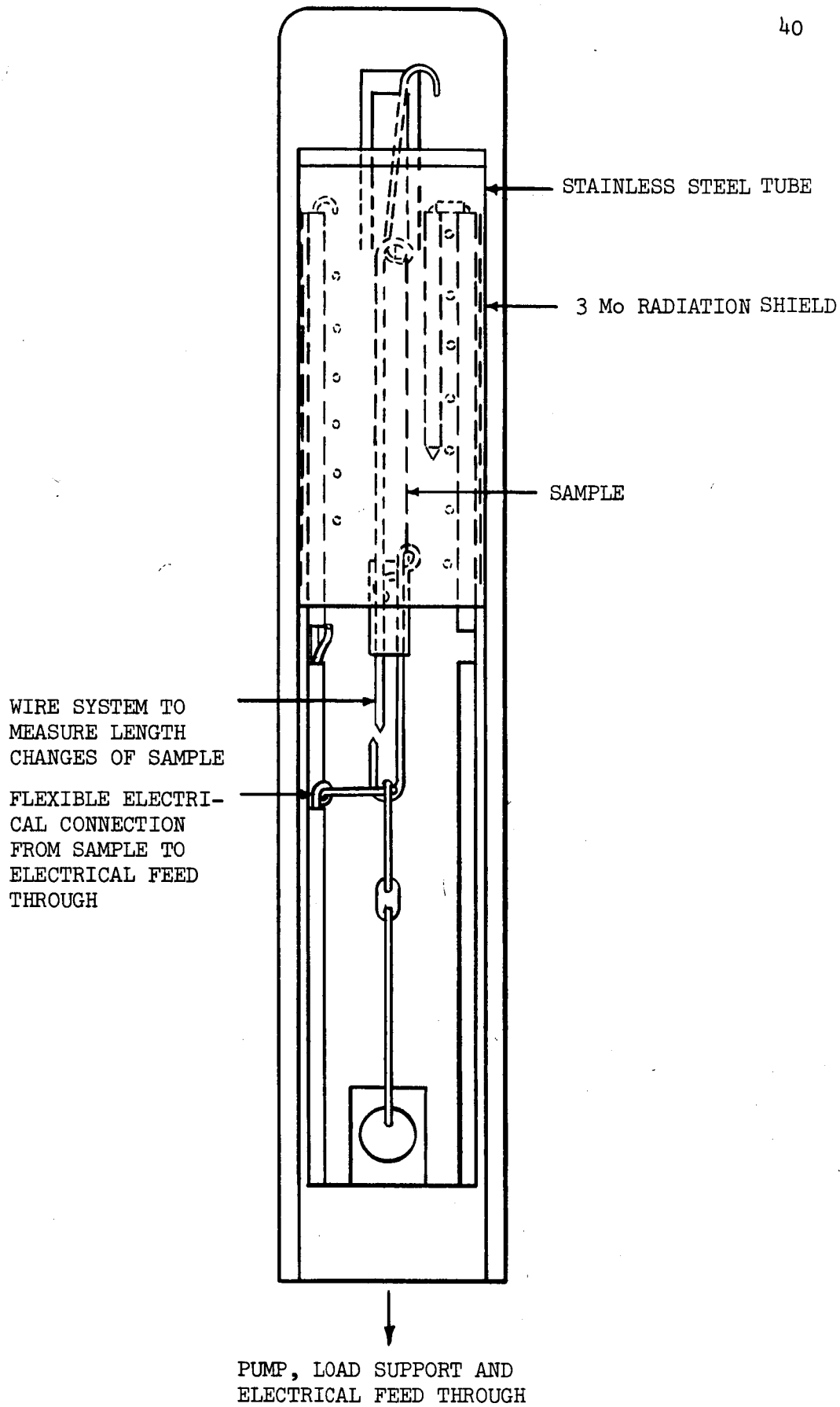


FIG. 15 SCHEMATIC DIAGRAM OF TEST SECTION

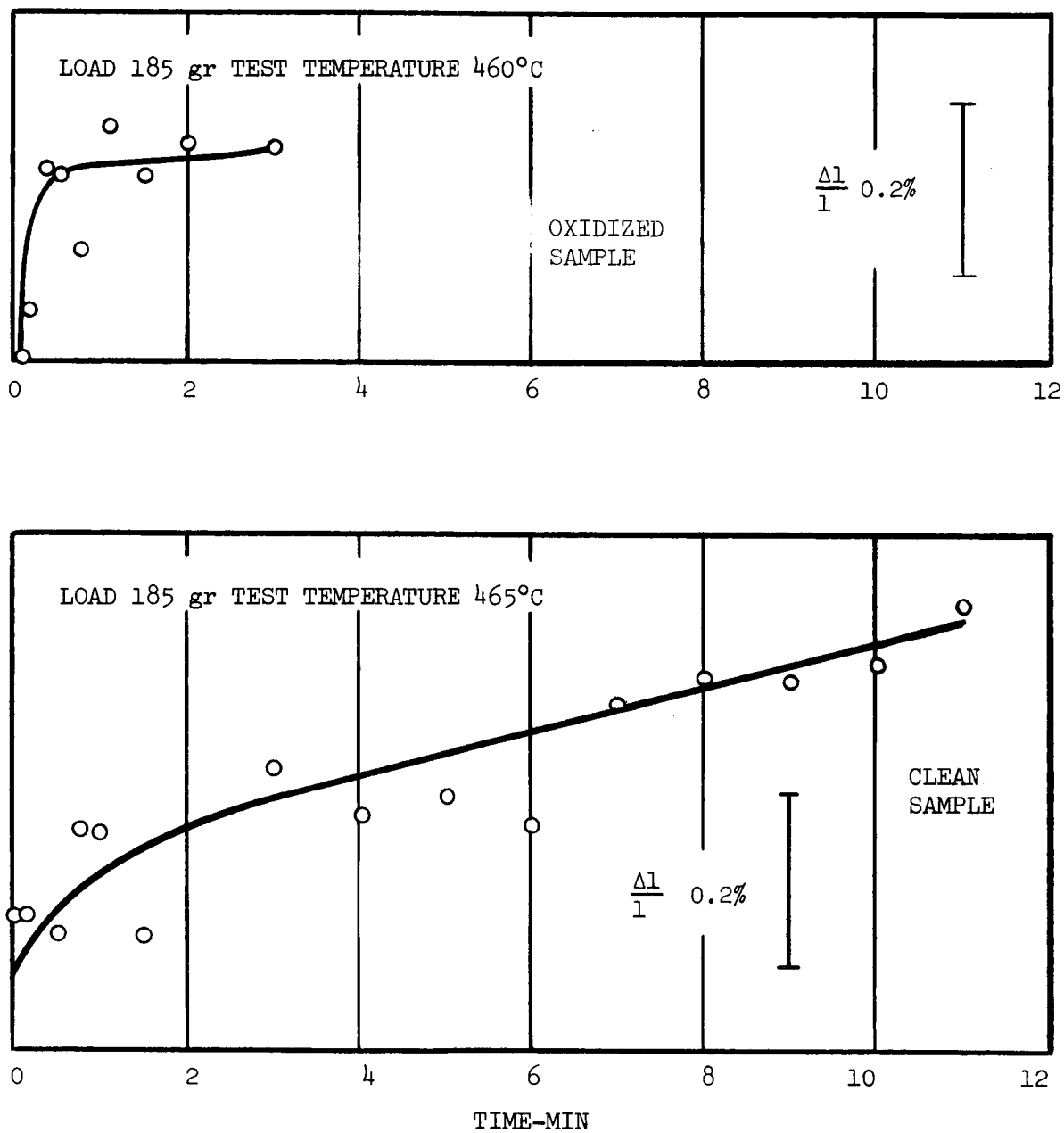


FIG. 16 CREEP TEST OF 0.008 INCH Cu WIRE SPECIMEN CLEANED AND TESTED, THEN OXIDIZED AND TESTED

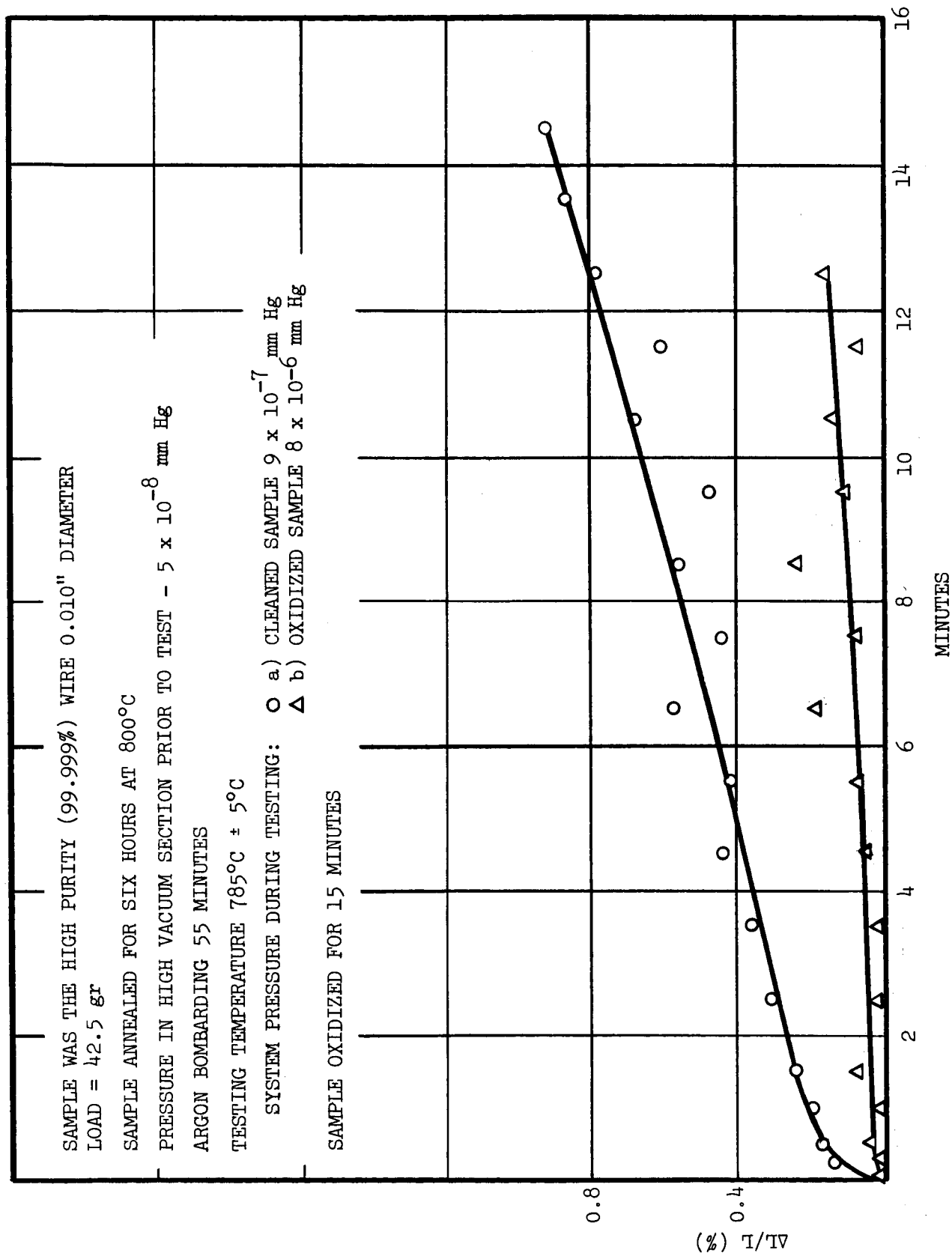


FIG. 17 CREEP TEST NUMBER 2 ON HIGH PURITY COPPER

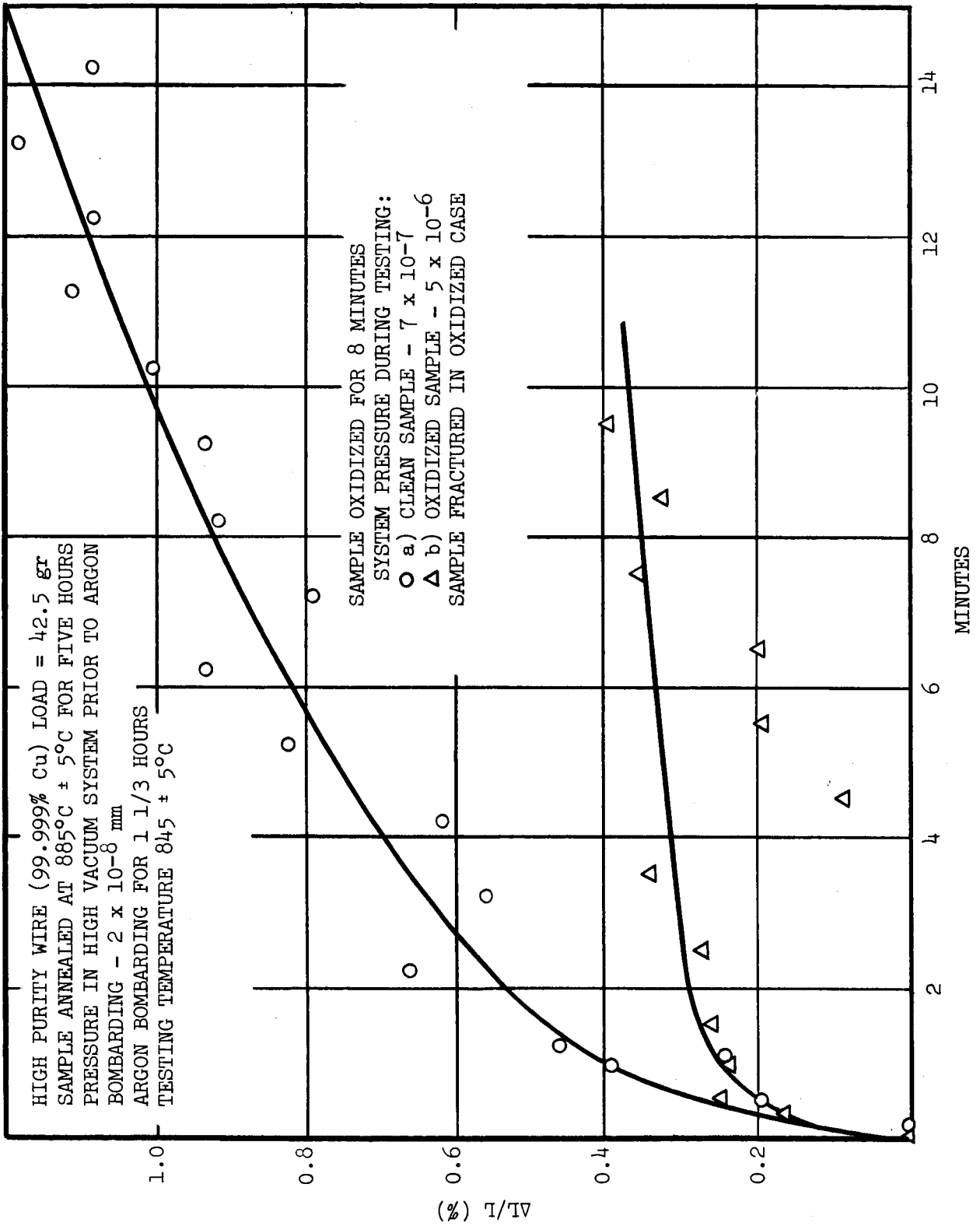


FIG. 18 CREEP TEST NUMBER 3 ON HIGH PURITY COPPER

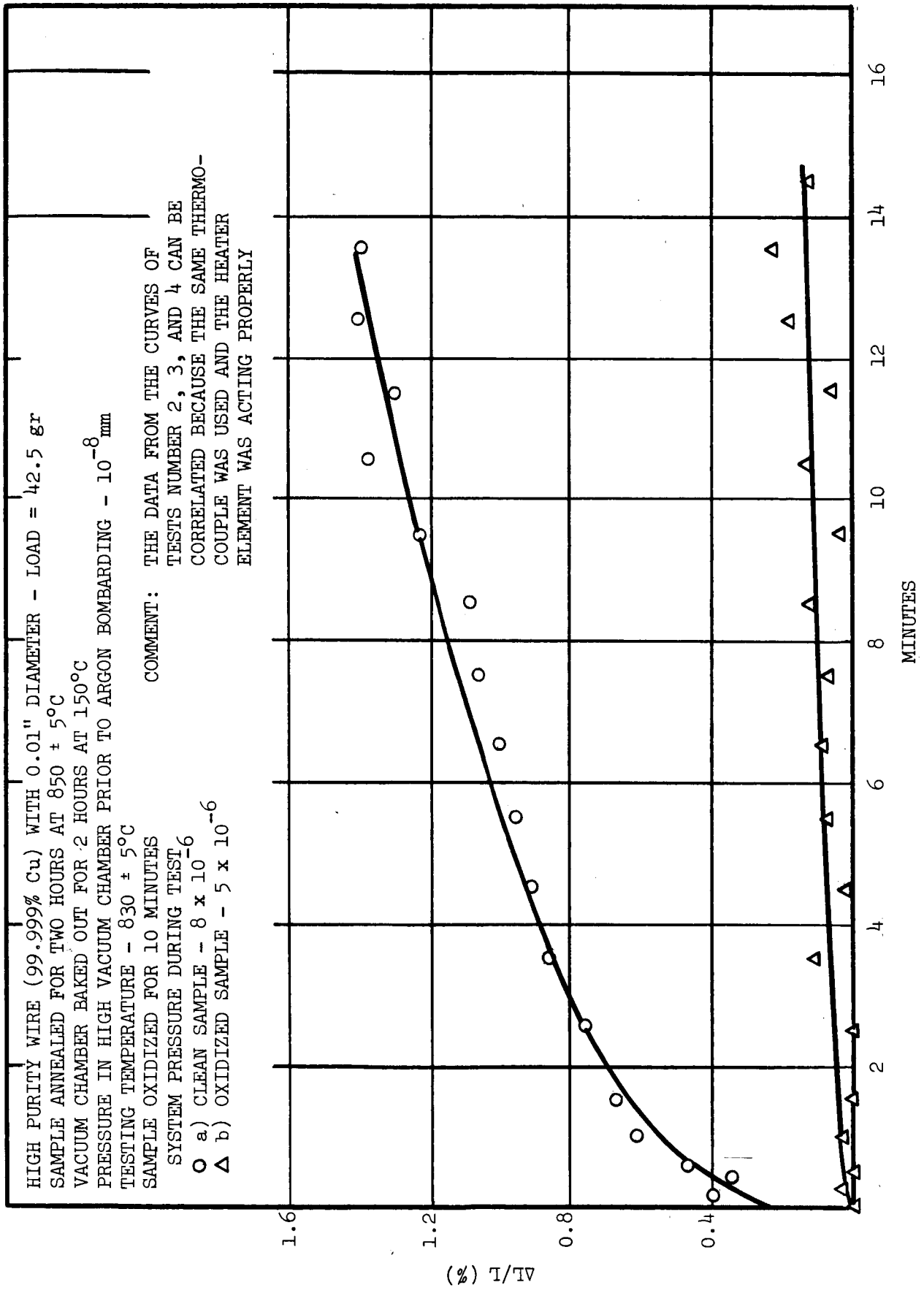


FIG. 19 CREEP TEST NUMBER 4 ON HIGH PURITY COPPER

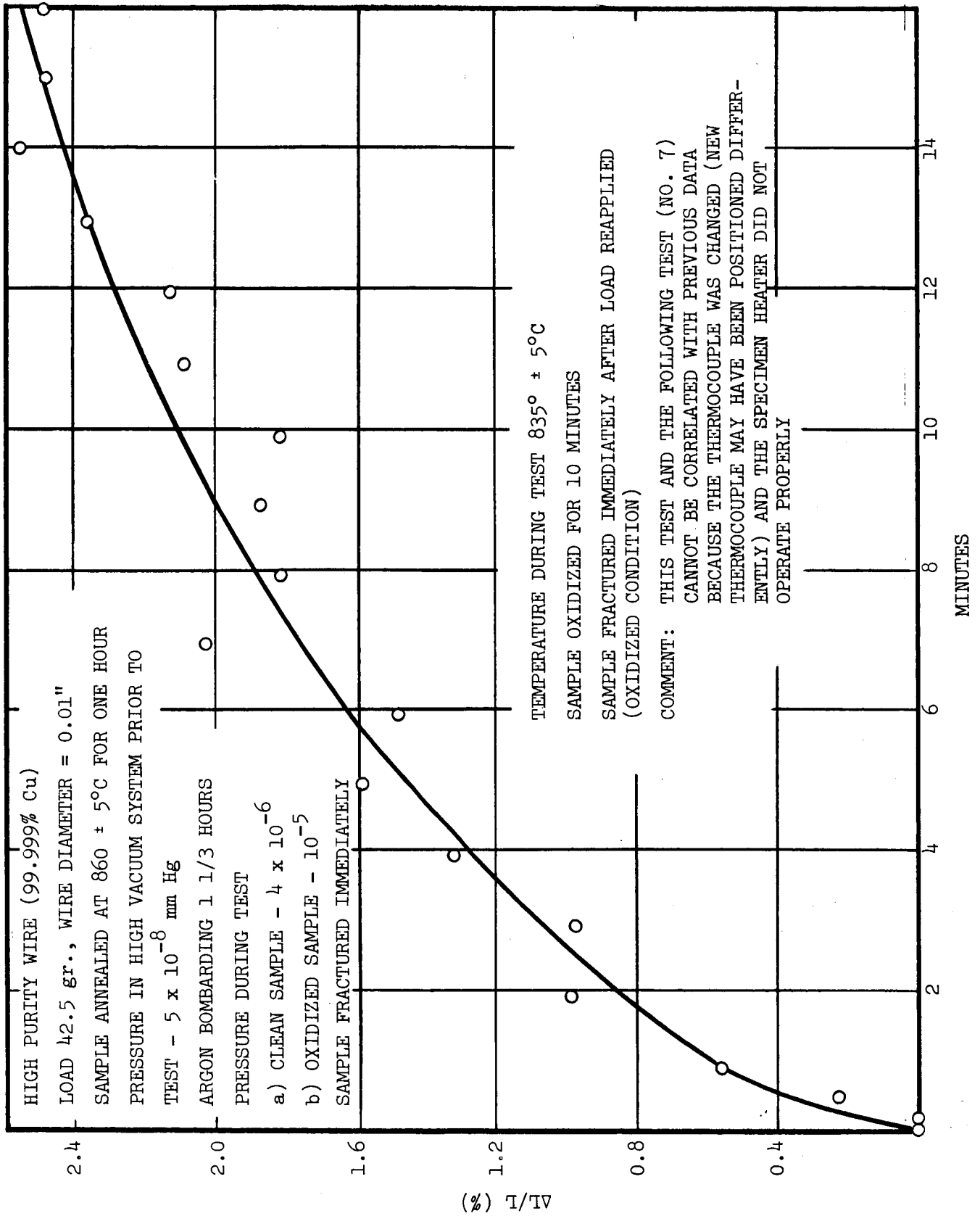


FIG. 20 CREEP TEST NUMBER 5 ON HIGH PURITY COPPER

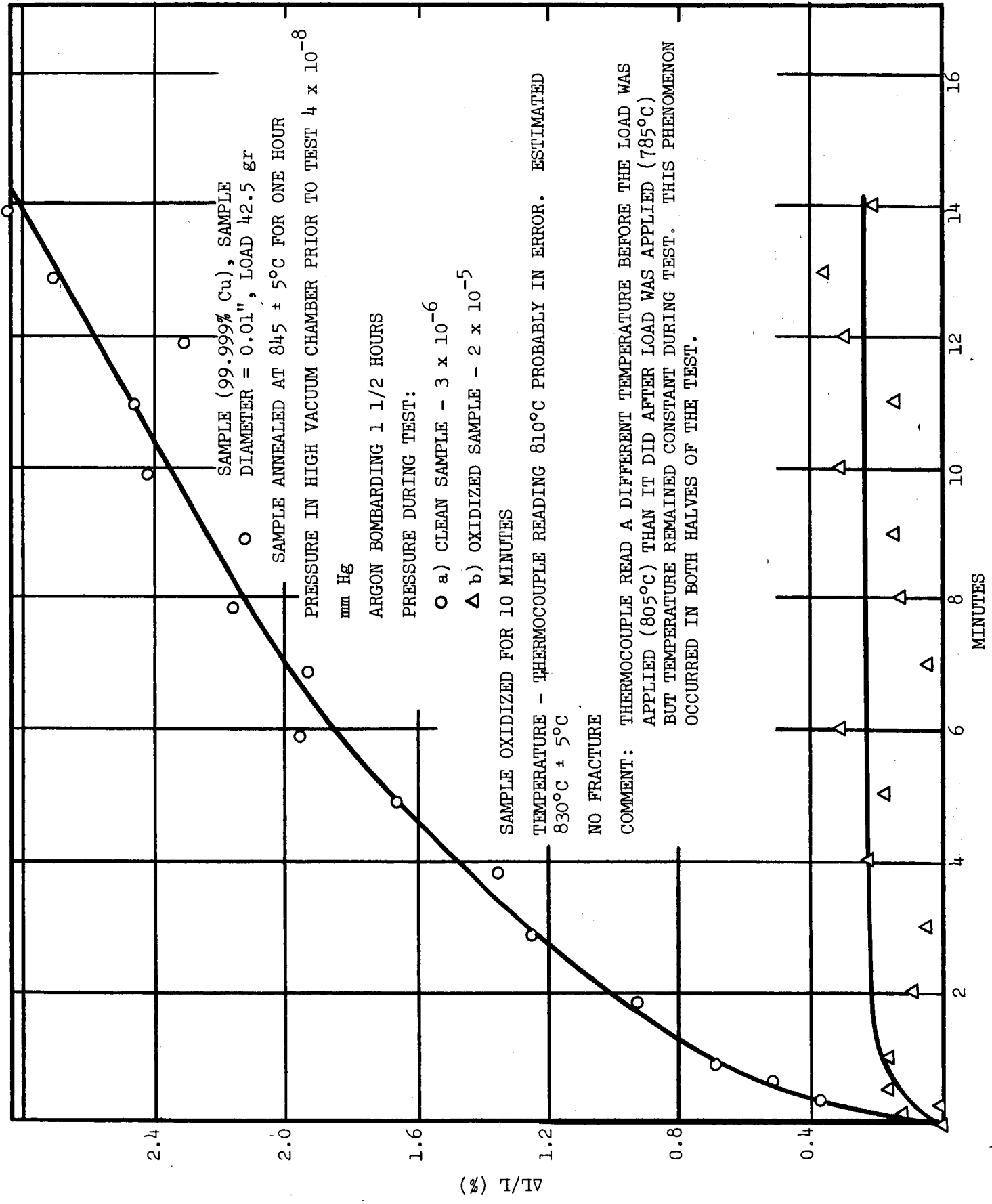


FIG. 21 CREEP TEST NUMBER 6 ON HIGH PURITY COPPER

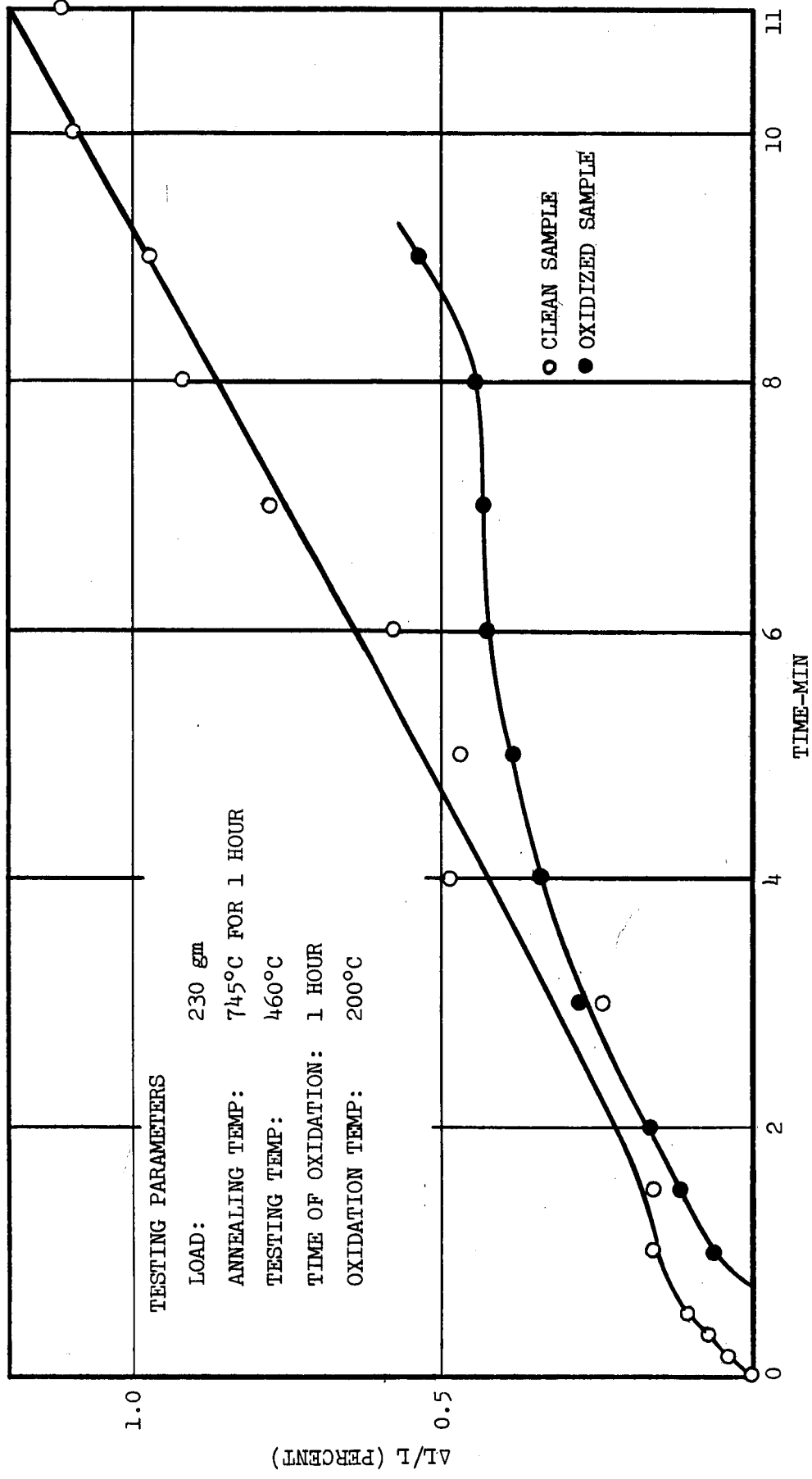


FIG. 22 CREEP TEST OF 0.008 INCH Cu WIRE OF 99.9 PERCENT PURITY

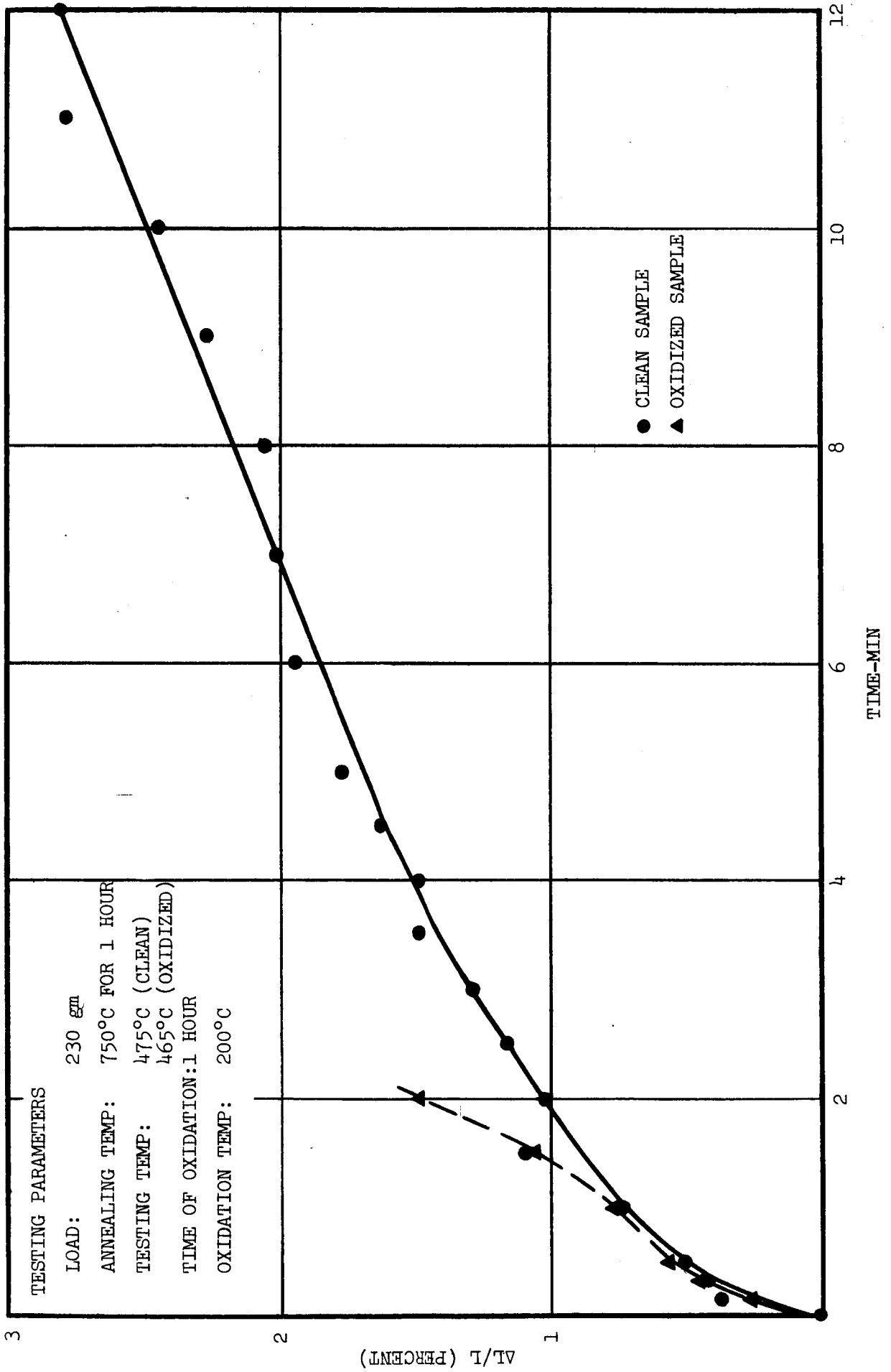


FIG. 23 CREEP TEST OF 0.008 INCH Cu WIRE OF 99.9 PERCENT PURITY